2015

Coal seam gas water treatment for beneficial reuse

Christian Elters
University of Wollongong

UNIVERSITY OF WOLLONGONG

Department of civil, mining and environmental engineering

Coal seam gas water treatment for beneficial reuse

CHRISTIAN ELTERS

This thesis is presented as part of the requirements for the award of the Degree of Master of Philosophy: Environmental Engineering

University of Wollongong

March 2015

ABSTRACT

Coal seam gas (CSG) extraction is widely practised in Australia and many other parts of the globe. The by-product of gas extraction is ground water and is commonly called CSG-produced water. The volume of CSG-produced water is large and is expected to rise, as the CSG industry in Australia and elsewhere continues to expand. The produced water is currently treated with reverse osmosis (RO) where both fresh water and brine are produced. The brine is 25% of the original water, and if the right extraction method is executed, further fresh water recovery is achievable. This study assessed the feasibility of CSG RO brine minimisation, by employing a pilot scale multi-effect distillation (MED) system. Samples were collected from two gas wells in Gloucester known as Craven 06 (CR06) and Waukivory 03 (WK03). Throughout the course of the study, the MED system was operated continuously at absolute pressure of 25 kPa. In each pilot evaluation trial, higher water recovery was attainable with water recovered from WK03 and CR06 greater than 95 and 97%, respectively. The MED performance showed near complete salt removal and distillate conductivity readings of 0.041 mS/cm and 0.022 mS/cm for WK03 and CR06, respectively. The distillate production was stable, averaging a flow rate of 16 to 17 L/h. The average feed flow rate was 21 L/h. High levels of thermal stability showed no evidence of scaling affecting the temperature inlet solution, with marginal decline in heat transfer coefficient, due to increasing the concentration ratio from eight to 10 times. The overall performance confirms that MED can be used for further treatment of CSG RO brine. The study recommends that concentrate from the MED to be reused for reclaiming minerals, to facilitate zero-liquid discharge and off-setting treatment costs (from the sale of suitable minerals i.e. sodium hydroxide or sodium bicarbonate).

ACKNOWLEDGEMENTS

My first acknowledgements are owed to the traditional owners of this land, the Wadi Wadi people. The thesis was accomplished on this sacred Country, and therefore, they must be acknowledged for. I hope this thesis benefits the traditional custodians, as it is to me, and the University of Wollongong (UOW).

My principal supervisor Prof. Long D. Nghiem, who has invested much of his time, knowledge, ideas and criticism for this study. All your efforts have made the dark stains of this thesis to shine like a bright mosaic. You have been a great teacher and support throughout the year. I thank you. I also thank my co-supervisor, Prof. William E. Price, for his immense and valuable support during my study.

A special thanks to AGL Upstream Gas, Ian Shaw, David Schneider, and other AGL staffs at the Gloucester office, who had provided accommodation, technical support and resources to make this research possible.

I thank Osmosflo for providing the membrane filtration units and Sasakura Co. for the multi-effect distillation. Technical support from Taner Ozdemir and Wayne Taylor (Osmosflo) as well as Taguchi Tatsuya (Sasakura Co.) are gratefully appreciated. The study has been successful because of your supply in recourses and support personnel.

Peter Monaghan and Nathan Kettlewell, from the very beginning of my undergraduate days, you have supported, believed and assisted me with your time and talents. This accomplishment would not have been possible without you. I thank you.

Elizabeth Elters, my sister. I thank you for providing me with the much needed resources (i.e. your laptop). I also acknowledge your own sacrifice for the progress of this thesis. Money was saved on train fares.

Hung Cong Duong, I thank you for proof reading my thesis, and supporting me with my mathematical problems in membrane technology. I also thank you for introducing me to phở.

Kai Whitaker, I extend my acknowledgments to you, for your time proof reading and commenting on the final draft.

Wenhai Luo, I thank you for all my troubles with EndNote.

I would like to thank UOW's Geospatial systems analyst, Heidi Brown. Your assistance with geographic information was essential to adding beauty to this thesis.

I would also like to extend my gratitude to Melanie Hybinett. I am thankful for those lifts all to university, which have paved my way into postgraduate research. I thank you.

I thank my parents. I am grateful for your ongoing financial and moral support. I hope I've made you proud.

I thank Sts. Thomas Aquinas, Patrick of Ireland, Scholastica, Gabriel of Our Lady of Sorrows, Gemma Galgani, Isidore of Seville, Tatiana of Rome, Ursula and Wolbodo (patron saints of students and engineering) for their intersession on my behalf.

I thank God most of all. As a Catholic, I believe that great things are accomplished by the blessings of the Most High Triune God. Whether we believe or not, His hand is always with us, entrusting to us His angelic hosts, who walk with, comfort and protect us. We should never forget these blessings. This thesis has been completed and is offered "Ad maiorem Dei gloriam" – To the greater glory of God.

TABLE OF CONTENTS

LIST OF FIGURES

LIST OF TABLES

CHAPTER 1: INTRODUCTION

1.1 Introduction into coal seam gas water

Coal seam gas (CSG) produced water is a by-product of the extraction of methane gas from underground coal seams. CSG-produced water often contains a high level of dissolved salts. Unlike produced water from off shore oil and gas exploration, which may be discharged directly to the ocean, CSG production occurs inland and CSG-produced water discharge into inland fresh water bodies would be detrimental to the environment [1]. Furthermore, recent studies have shown potentially detrimental effects on soils, plants and aquatic life due to exposure to untreated CSG-produced water [1, 2]. Thus, careful management of CSG-produced water is required prior to environmental discharge or any form of beneficial usage.

The production rate of CSG-produced water varies over the lifespan of the gas field. The generation of produced water peaks in the first two years of gas extraction, then declines (as gas production increases). CSG exploration and production have increased in the past decade and will continue to increase as energy demand rises [3]. CSG water is produced at a rate of 75,000 ML/year in Australia, which is equivalent to 30,000 Olympic size pools [4]. Hence, redirecting CSG-produced water for sustainable use is essential.

Reverse osmosis (RO) is widely used for treating CSG-produced water. However, pressure restrictions mean that only a fraction of fresh water can be recovered. Evaporation of the remaining waste water (called RO brine) yields ionic solids, which are collected and transported for further processing [5, 6]. The evaporation takes place in an evaporation pond. Evaporation ponds have become unlawful in most states of Australia [7], because the plastic lining can erupt and leak out the brine. Since this discovery, authorities have actively encouraged CSG operators to phase out evaporation ponds, and develop new technologies to minimise brine. Multi-effect distillation (MED) is a desalination technology that can potentially treat the CSG RO brine. MED has been widely used for seawater desalination in China,

the USA and various Arab nations. MED is capable to treat CSG RO brine, because the salt content is much lower compared to seawater. In addition, the distillation process is not restricted by osmotic pressure, thus, CSG RO brine minimisation is foreseeable. The main disadvantage to MED is the requirement of heat energy. However, literature have reported developments in MED that can reduce energy consumption [8]. This study will investigate the MED for its feasibility in minimising CSG RO brine.

1.2 Project aims

This study will minimise CSG RO brine using a single-effect MED system. The study also expects the MED to be suitable for the management of CSG brine, other than the conventional evaporation ponds.

The main objectives in this study are as follows:

- Demonstrate the treatment of CSG-produced water in Gloucester, NSW, Australia. The produced water will be treated using a pilot scale MED system, and water recoveries set between 80 to 90%. From here, laboratory analyse will be conducted to examine the distillate purity. The distillate will be produced from RO brine.

- The feasibility will be assessed by the MED's performance, characterised by distillate production, rejection of contaminants and the thermal stability.

- Assess the feasibility of brine minimisation with respect to CSG-produced water quality.

1.3 Thesis outline

This thesis consists of 5 chapters. The schematic diagram in Figure 1 illustrates the thesis structure. Chapter 1 describes the projects aims, outlook and potential research gap.

Chapter 2 provides an extensive literature review. In the review, it is centred on the future technologies for minimising RO brine. The literature review also highlights extractable minerals and potential use of CSG water.

In chapter 3, the origin of the associated water is discussed for the individual gas-well. Chapter 3 also details field work, laboratory analyses and distinguishes the pilot protocols executed for samples collected on November 2013 and March 2014.

Chapter 4 expands and compares the data collected from each pilot evaluation program in November 2013 and March 2014. This chapter is outlined in the following order: (1) characteristics of WK03 and CR06 CSG-produced water (2) comparing Gloucester's produced water to other CSG-produced waters (from Bowen Basin, QLD, Australia) (3) performance of membrane technologies: ultrafiltration (UF) and RO (4) performance of MED further treating RO brines and (5) the feasibility of MED and permeate and distillate discharge suitability (fit-for-purpose).

The conclusion and recommendation for future work is summarised in chapter 5.

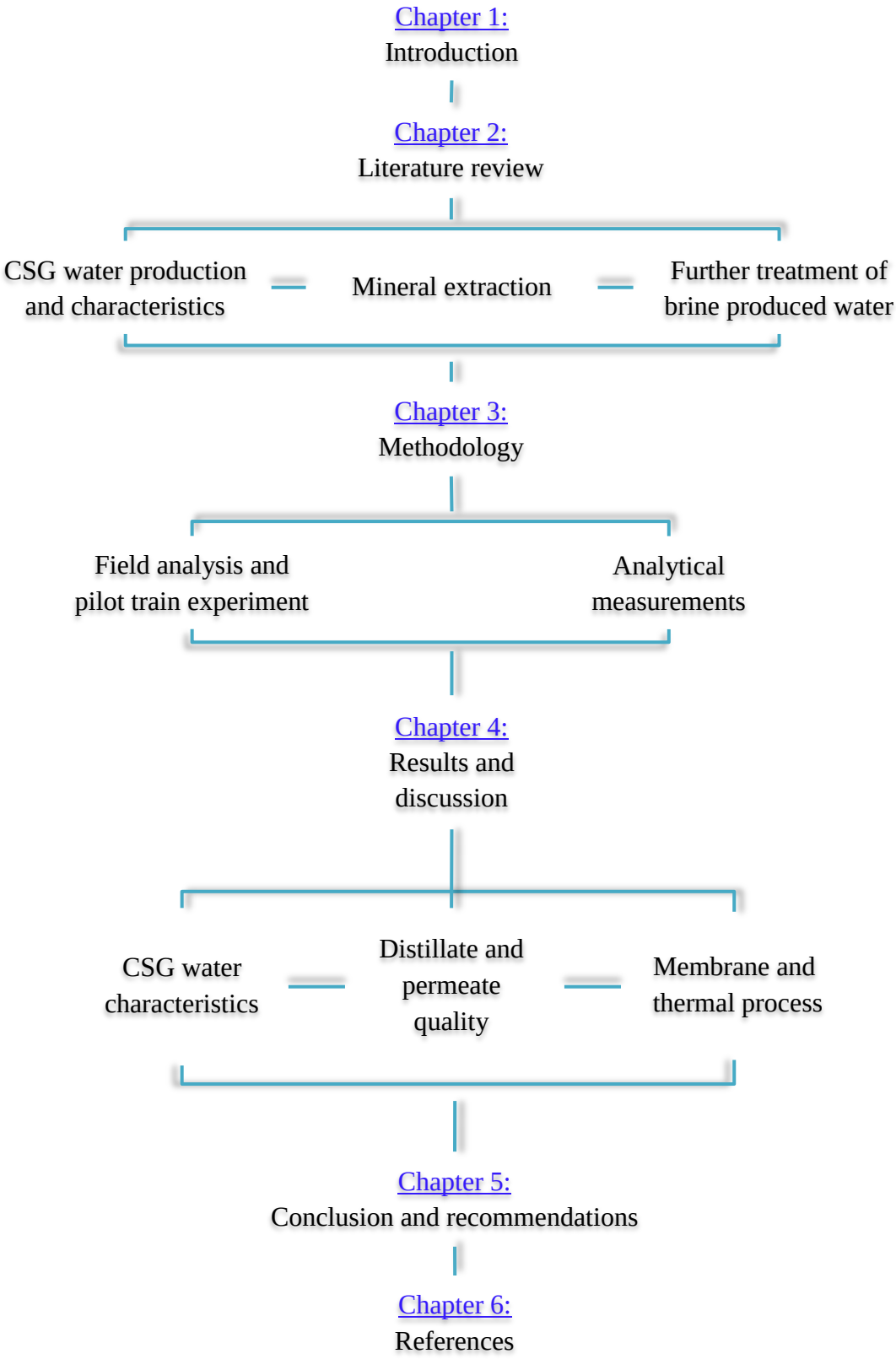

Figure 1: Overall structure of the thesis.

CHAPTER 2: LITERATURE REVIEW

2.1 Coal seam gas

Coal seam gas (CSG) is a natural gas (methane) that can be extracted from underground coal seams. CSG is located several hundred meters below the surface (Figure 2), and is usually absorbed onto coal seams, organic particles and the surrounding formation waters [3, 9]. Coal seams contain a large volume of gas, and thus is a very significant energy source [9, 10]. For example, Australia's Origin Energy Combabula gas field in the Wandoan area, QLD, produced 71 billion m^3 of CSG in the 2012-13 financial year [11]. Proven CSG reserves in Australia, North America and Russia are 3.8, 10.8 and 32.9 trillion m^3, respectively [12].

The power sector has high energy demands, which consumes 21% of the global gas supply [10]. The demand for natural gas is growing at a rate of 1.6%, annually, and by 2035, the gas supply will increase to 5,000 billion m^3. China's increasing population and economy is attributed to this high demand, and by 2035, China will import most of the globe's natural gas; importing one-third of the world's natural gas supply [10].

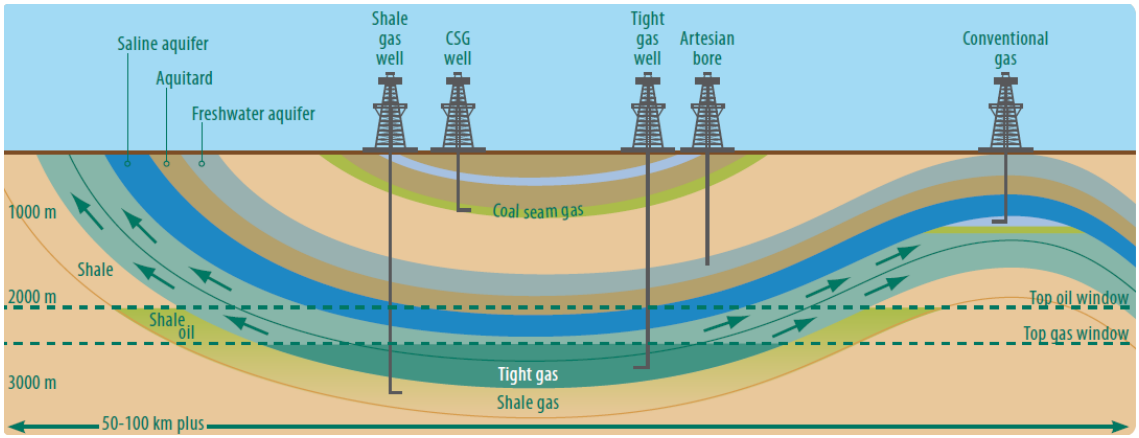

Figure 2: A typical setting for CSG formation (from [9]).

Australia has been exploring and exporting CSG since the 1970s and 1996, respectively. Most of Australia's CSG is extracted from QLD's Surat and Bowen Basins, while a fraction is produced in NSW. In the 2010-11 financial year, 6.4

billion m^3 of CSG was produced in QLD, while 0.16 billion m^3 were produced in NSW. During 2010-11 financial year, 97% of Australia's CSG was produced in QLD [13]. Since 2009, Australia has exported two-thirds of its liquefied natural gas to Japan, and the remaining to China and Korea. The gas export for 2009 was 4 billion m^3. Figure 3 illustrates the supply of CSG from Australia's Surat and Bowen Basins [3, 10, 14, 15]. If CSG production is to remain steady, the life expectancy of this industry will last for 100 years, which is longer than oil, black coal and conventional gas [16].

CSG is released from the coal seams when the surrounding water is pumped out. This process must be done first to depressurise the seams, which results in desorption of CSG from the coal bed [3, 17].

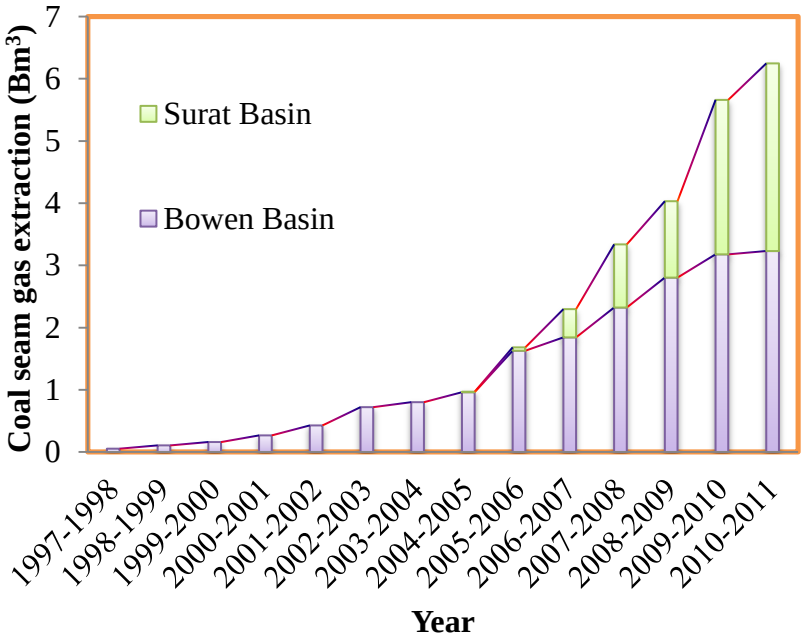

Figure 3: Coal seam gas extraction from Surat and Bowen Basins (Adapted from [11]).

2.2 Coal seam gas produced water

2.2.1 Water characteristics

CSG-produced water is dominated by Cl^-, Na^+ and HCO_3^- with minor trace elements [3, 18-20]. Van Voast [21] reported Ca^{2+} and Mg^{2+} concentrations in CSG-produced water are inversely proportional to HCO_3^- concentration. The presence of HCO_3^- will precipitate Ca^{2+} and Mg^{2+} to form $CaCO_3$ and dolomite ($CaMg(CO_3)_2$). Table 1 illustrates common characteristics of CSG water from various basins around Australia and the USA. Factors associated with CSG water depends on the coal seam depth, rock composition and the surrounding coal seams, age of surrounding water and the origin of the water associated with the coal seams [3], which influences water characteristics from one basin to another. For example, trace elements from five different watersheds in USA's Powder River Basin were analysed. Among the trace elements analysis, Al^{3+} showed greatest discrepancy with concentration between 0.18 to 1.82 mg/L from the five watershed locations [22]. In another study by Jackson and Reddy [23], pH, electrical conductivity, Ca^{2+}, Mg^{2+}, Na^+, and alkalinity were analysed from the same watersheds from their previous study. Their results showed electrical conductivity, Ca^{2+}, Mg^{2+}, Na^+, and alkalinity can vary significantly whereas, pH, was the most stable parameter from the five watersheds.

Ion-exchange is also responsible for depleting Ca^{2+} and Mg^{2+}. In coal aquifers, groundwater comes into contact with Na-containing minerals. Ion-exchange occurs, and the Ca^{2+} and Mg^{2+} ions are sequestered in clays, while Na^+ concentrations in the water increase. In aquifer recharge areas, the water is fresh with low total dissolved solids (TDS). As an aquifer depth increases, the chemistry of the water changes [18]. TDS in Australian CSG water ranges from 1,000 – 6,000 mg/L [3]. Such levels exceed the nationally allowable limit for irrigation, as defined by the Australian Standards. Native flora and fauna can be at risk if the water is left untreated: this is a consequence of the high ionic content [3]. High HCO_3^- content, in particular, decreases the solubility of plant nutrients. TDS in seawater is 30,000 – 40,000 mg/L, which is (on average) 10 times greater than CSG-produced waters [24].

Table 1: Coal seam gas water quality in well sites around Australia and USA [3, 25, 26].

	USA		Australia		
Water Chemistry	**Powder River (Wyoming)**	**Raton Basin (Colorado)**	**Surat Basin (Tipton)**	**Gloucester Basin (WK03)**	**Gloucester Basin (CR06)**
Physicochemicals					
pH (-)	7.71	8.19	8.25	7.6	7.84
TDS (mg/L)	997	2,512	5250	2,918	4,385
TSS (mg/L)	11	32.3			
SAR (meq/L)	16.2	72.2		74.4	119
Inorganic					
$CaCO_3$ (mg/L)	1.384	1,107	1030	2,100	2,020
Al^{2+} (mg/L)	0.018	0.193		0.06	0.01
HCO_3^- (mg/L)	1,080	1,124		2,100	2,020
B^{3+} (mg/L)	0.17	0.36		0.19	0.27
Ca^{2+} (mg/L)	32.09	14		7	9
Cl^- (mg/L)	21	787	2060	437	1,270
Cu^{2+} (mg/L)	0.078	0.091		0.001	0.001
F^- (mg/L)	1.57	4.27	0.885	0.3	1.4
Fe^{2+}/Fe^{3+} (mg/L)	1.55	7.18	2.29	27.2	37.8
Mg^{2+} (mg/L)	14.66	3.31		2	4
Mn^{2+} (mg/L)	0.02	0.11	0.085	0.32	0.475
Silica (mg/L)	6.46	7.05		19.9	13.7
Na^+ (mg/L)	356	989	2650	1,230	1,710

Note: Values given from Gloucester Basin were sampled on 13/08/2013 and are not given as averages. USA entries are averages, and; SAR, Na^+, Ca^{2+} and Mn^{2+} have units of meq/L. Surat Basin pH, TDS, Na^+, Fe^{2+}/Fe^{3+}, Mg^{2+} and F^- are given as average.

The sodium adsorption ratio (SAR) measures the adsorption tendency of Na^+ at ion-exchange sites, where other ions are available (e.g. Ca^{2+} and Mg^{2+}). This parameter is represented as a ratio of Na^+ to Ca^{2+} and Mg^{2+} in soils [27, 28]. The following equation is used to calculate the SAR:

$$SAR = \frac{[Na^{+}]}{\sqrt{1/2\left(\left[Ca^{2+}\right]+\left[Mg^{2+}\right]\right)}} \quad \text{Eq. 1}$$

When the SAR is high, Ca^{2+} and Mg^{2+} ions in soil profiles is low compared to Na^{+} [15]. In this instance, the soil physical properties such as structure, permeability and hydraulic properties will deteriorate [4, 15-17]. For example, two silt loam clays contained in high Na^{2+} water, were measured for soil structural permeability. The results conveyed maximum decrease in permeability when SAR was SAR ≥16 and SAR ≥ 8 [29]. In another study [30], structural breakdowns of soil profiles were reported, when the SAR was 15. The structural breakdowns were a result of increasing swelling forces in the aggregate [30]. Overall [27], vegetation irrigated with high SAR water is not suitable.

2.2.2 Water production

In the initial CSG production phase, a large volume of produced water is generated, which then decrease as the gas production carries on, over time [3, 20, 31]. For example, a gas-well in 1999 generated 0.046 ML/day of produced water in the Powder River Basin, USA. From 2000 to 2001 the water production decreased from 0.031 to 0.021 ML/day, respectively [32]. Figure 4 shows a typical water and gas production profile from a gas-well. The water decreases as the lifetime of a gas-well continues, because of depleting water recourses from the gas-well.

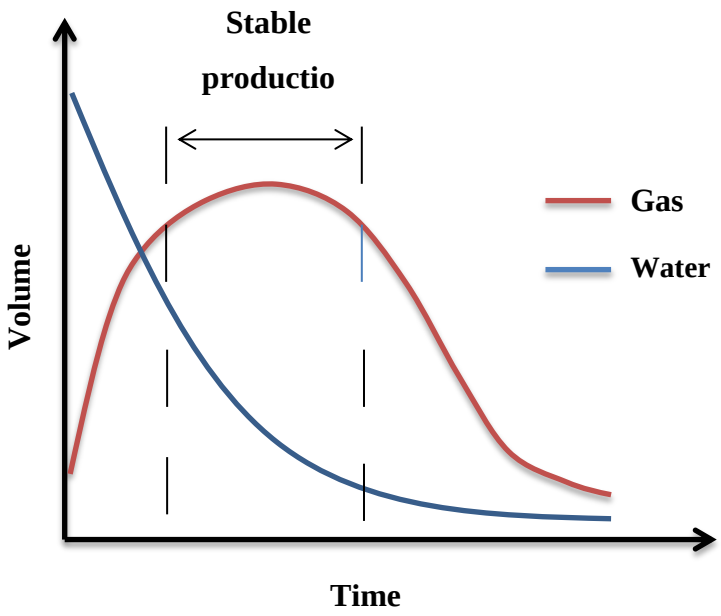

Figure 4: Production curve of a typical CSG well as a function of time.

In each gas-well the production of water can vary significantly, which is dependent on the basin geology and water pressure [20]. For example, a gas-well in Fairview's Bowen Basin, QLD, produces 0.02 ML/Day of produced water, while water production from another gas-well, yet in the same field was 21 ML/day. The water production varies for a number of reasons, such as duration of CSG production, depths of coal seam burial, the type of coal and hydraulic settings [3, 20, 33].

2.2.3 Water management

Evaporation ponds have been the primary method for disposing CSG water. In 2010, this method was banned, due to leaching of produced water (by chance of the torn pond lining) and contaminating the groundwater. However, alternative methods have been considered for disposing CSG-produced water [7, 31]. These options include reclaiming water for beneficial reuse (see section 2.2.4 and 2.2.5) and disposing into waterways. CSG water disposed into waterways will require precaution, so that environmental values are respected, limiting any impact to ecological settings. Although evaporation ponds have been discontinued, some exceptions have been granted for new CSG operating wells. The approval may be granted if an alternative management practice is not achievable [7]. Current CSG operators are required to

continue decommissioning evaporation ponds, as outlined in the 2010 CSG water management policy.

2.2.4 Beneficial use of coal seam gas water: growing algae, livestock use

CSG-produced water can be put into beneficial practices such as irrigation, livestock use, potable water supply, coal washing and industrial operations [34]. Although research reports using CSG water for irrigation will reduce the water availability to crops, because of the substantial salt content [15], others have shown it to be useful in harvesting peppermint and spearmint [35]. When blended with 50% fresh water, the peppermint and spearmint harvests yielded good compositions with essential oils and antioxidant activity. The total spearmint and peppermint herbage yield were 427 and 583 grams/pot. The composition of CSG water used was not specified.

CSG water has shown to be feasible at cultivating algae. Algae cultivation is more cost effective compared to conventional desalination technology, which could be used as another means for disposal of produced water [36, 37]. Algae were grown in untreated (TDS 1.7 g/L) and treated CSG water (TDS 11.6 g/L). The untreated water showed success while the treated water had a harvest that lagged nine times in yield [38]. Another study investigated algae growth with CSG water containing high HCO_3^- ions. The study produced 24% of algae growth from a dry mass content in five days [36].

2.2.5 Mineral extraction

CSG brine contains dissolved minerals that can be remediated with techniques patented for sea salt recovery. Mineral reclamation not only benefits ecology but also the economy [39, 40]. Pure brine remediated by precipitating minor constituents is possible. For example, Mg^{2+} and Ca^{2+} reacted with ammonia and phosphoric acid will precipitate out of solution as magnesium ammonium phosphate and calcium hydrogen phosphate, to leave a more pure solution (NaCl for example) [39]. This technique is proven for seawater and waste water RO brines, but research into

mineral reclamation from CSG brine is yet available. Melián-Martel et al.,.[41] and [42] investigated the production of NaOH (also called caustic soda) from seawater RO brine using a semipermeable membrane electrolysis cell. The results showed that it is possible to produce NaOH with strength of up to 32% w/v by membrane electrolysis.

Recently, Simon et al. [43] extracted NaOH from CSG RO brine, using a membrane electrolysis cell. In their study, Na_2CO_3, $NaHCO_3$ and NaCl were used for feeding the cell, to precipitate NaOH. The results showed little difference in NaOH from the three feed source (100 mg/L). The NaOH produced was 12 and 18% from Na_2CO_3 and NaCl, respectively [43].

NaCl is a main component in manufacturing Na_2CO_3 (soda ash), and a typical process for producing soda ash is the *Solvay process*. Literature has not shown soda ash conversion from CSG-produced waters to be feasible. However, oil-produced waters have shown the Solvay process to be effective. Results from [44] exhibited soda ash production from raw oil-produced water with 83% purity.

In 2012, Penrice Soda and General Electric (GE) announced its pilot scale plant for remediating soda ash, $NaHCO_3$ and salts from CSG-produced waters. This was to demonstrate the feasibility of remediation before establishing a commercial plant [45]. The current status on the pilot scale project is unknown, and the proposed commercial plant is still to be announced.

2.2.5.1 Market for soda ash and caustic soda

2.2.5.1.1 Soda ash

Soda ash is an important mineral, where 30% is produced naturally from the mineral trona (or Na_2CO_3 bearing brines), while 70% is made up synthetically [46]. It is used to manufacture chemicals, glass, soaps, detergents, paper and pulps. Soda ash is highly demanded in manufacturing flat glass sheets, which requires 50% of the global demand, due to the emerging construction and automotive industry [47-49].

China is the highest producer and consumer of Soda ash. China produces 45% of the global demand and consuming 43% of this [49, 50].

Penrice Soda is Australia's only producer of soda ash, with a capacity to produce 100,000 tonnes, annually. However, in the last three financial years, Penrice Sosa had exceeded their capacity, producing 310,000 tonnes for each subsequent year [50]. Recently, Penrice Soda have turned its venture from manufacturing to importing, because of financial downturn [51]. Australia's market value for soda ash (99% purity) is $AU360 per metric tonne [52]. Because of economic downturn in Australia's only soda ash producer, CSG operators would risk converting CSG brine into soda ash, because it does not trade.

2.2.5.1.2 Caustic soda

Caustic soda is used to manufacture chemicals, soaps, detergents, wastewater treatment, ceramics, glass, paints and textiles. The globe demands 40% of its caustic soda for chemical manufacturing. Two other end users such as alumina production and pulp and paper sits second on the global demand, requiring 30% of the caustic soda supply [53]. Australia has the world's largest alumina industry and relies on caustic soda exports from Japan, to maintain its alumina production. Japan currently holds 8% of the world's caustic trade [54]. Caustic soda can be remediated from CSG brine [43], and would be valuable to the alumina industry. Caustic soda is making soda ash redundant in the glass and paper and pulp industry, because processing caustic soda is much cleaner and easier to handle compared to soda ash [55]. The current price on caustic soda is averaged $AU350 per metric tonne (50% purity) and $AU750 per metric tonne (99% purity) [52].

2.3 Reverse osmosis

Reverse Osmosis (RO) is a desalination technology that uses a semipermeable membrane to separate dissolved ionic compounds from fresh water. In RO, pressure is the main driving force of the process, and is applied at levels beyond the osmotic

pressure of water on the membrane containing high dissolved ionic substances. The applied external pressure allows for the passage for water in high saline solution to migrate to low salt water (Figure 5) [56]. RO is capable in recovering 75% of fresh water from the feed water source.

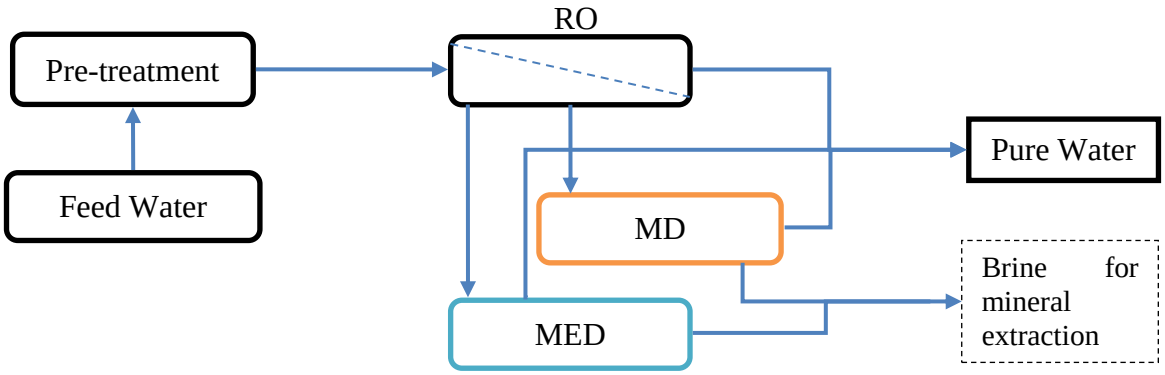

Figure 5: Schematic diagram of an RO unit coupled with MD and MED unit for CSG RO brine treatment.

RO is most popular for sea and brackish water desalination. It is also used for treating household wastewater. RO is also the treatment technology of choice for CSG water, because it is a cost-effective process and continuously improving in configuration and water processing (Table 2) [3, 57]. These improvements are the result of RO popularity, which has also reduces operational and capital costs [58]. For example, a spiral wound membrane was limited to 70 bar of applied pressure. Today, RO can apply 83 bar to the spiral membranes. This increased the water recovery to greater than 60% [59]. Applied pressure and permeate recovery improvements, were the result of better membrane stability and permeate spacer technology.

Table 2: Capital and operating costs (AU$) of several desalination technologies [3].

Technology	Capital Costs	Operating Costs
MSF	2,000 – 3,800	Depends on energy cost
MED	2,500 – 3,900	1.8 - 2.8
VCD	1,600 – 1,700	Depends on energy cost
RO	700 – 1,000 (brackish water)	0.65 - 1.5 (brackish water)
	1,700 – 2,400 (seawater)	1.89 - 2.2 (seawater)
ER	570 – 3,250	1.00 - 2.80

MSF: multi-stage flash; MED: multi-effect distillation; VCD: Vapour compression distillation; ER: Electrodialysis reversal.

The RO brine is disposed in a storage dam (only for current and not new CSG projects, which are required to substitute evaporation ponds, with another water management plan), and left to evaporate. However, technologies are available to further treat RO brine. These technologies are MED and membrane distillation (MD). The net driving force in RO is limited due to the concentrate osmotic pressure. However, in MED and MD this is not a factor in the distillation process [60, 61], hence the increased water recovery. Sections 2.4.1 and 2.4.2 will discuss MED and MD in detail.

Spring Gully, QLD, was the first CSG mine to integrate RO into the CSG production (Table 3). The RO has a treating capacity of 9 ML/day and is set to 75% water recovery. An estimated 5.9 ML/day of produced water is generated from the 10 operating wells, which yields 4.4 ML/day of treated water [62]. RO systems used in various CSG fields, in Australia and the USA, are summarised in Table 3.

Table 3: Types of treatment processes employed for CSG water treatment [3].

Facility	Capacity (ML/d)	Year	Location	Processes
Wild Turkey	20	2006	Wyoming	Multimedia filter – RO
Spring Gully	9	2007	Queensland	Sand filtration – MF – RO
Mitchell Draw	12	2008	Wyoming	Multimedia filter – IX – RO
Gillette	5	2008	Wyoming	Zeolite pre-filtration – IX

2.4 Technologies to further treating reverse osmosis brine

2.4.1 Multi-effect distillation

MED is the oldest of four desalination processes employed commercially. The other three processes are multi-stage flash (MSF), multi-effect vapour (MEV) and RO [63]. Unlike RO, MED is a thermal process involving phase change from water to vapour. MED consists of multiple effects (evaporation phases) where, in each consecutive effect, the temperature boiling point (pre-heated horizontal tubes) is lowered, due to increased vacuum pressure in each subsequent effect. Figure 6 illustrates the design concept of three effects.

Seawater is raised to rapid boiling point in the first effect and sprayed onto the preheated horizontal tubes, by an external thermal source. The seawater that remains unevaporated is continually transferred to the next effect to undergo evaporation. The horizontal tubes are heated in each effect by the condensation of vapour from the last effect; the vapour condensed is stored as distillate. Latent heat is expelled from the condensation of vapour, which is used to evaporate seawater. The cycle of evaporation and condensation in each effect is repeated consecutively at lower pressure and temperature [64]. The concentrate in the final stage is fully condensed, ejected and stored [65].

MED requires 1.8 kWh/m^3 of energy to produce distillate, which is the result of the low boiling temperatures. This consumption rate is less than MSF, which consumes power at 4 kWh/m^3 [66]. In addition to low temperature, scaling by divalent ions is reduced (common problem in distillation and pressure driven processes). Feed water temperature greater than 75°C increases precipitation of scalants, which effectively reduces the heat transfer efficiency, and decreases the production of fresh water. Operating MED at low temperatures reduces the risk of scaling and maintains a steady production process [67]. MED can be operated below 70°C, making this a more energy efficient technique than other evaporation processes [68, 69].

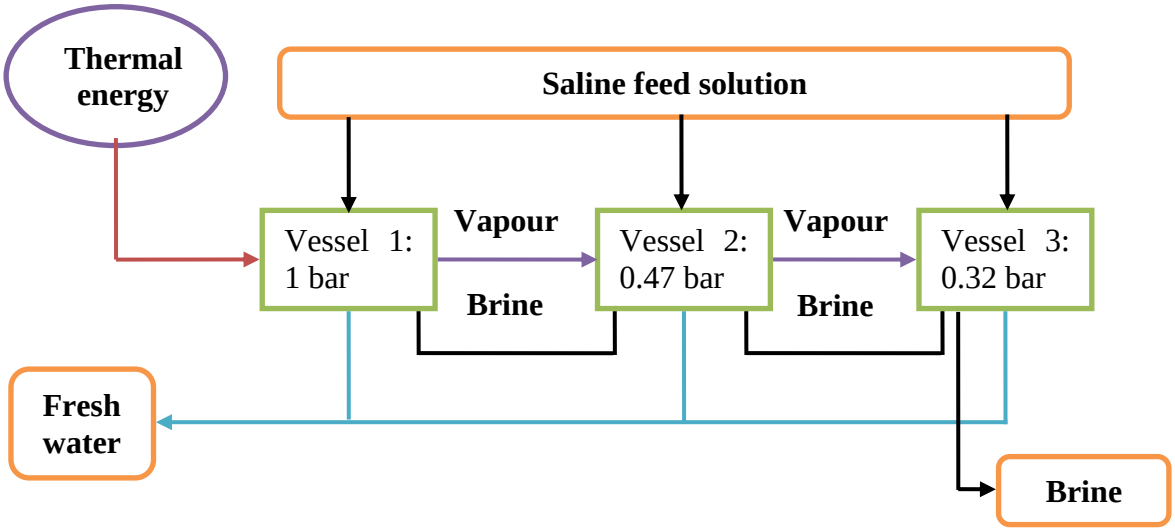

Figure 6: Schematic diagram of a MED unit with effects. The first vessel (or effect) is heated with an external energy source while, each consecutive vessel, the temperature of boiling point is raised, by latent heat, released by the condensation of vapour. The vacuum pressure in successive evaporation vessel is reduced to lower the boiling.

There is no literature on MED and CSG water treatment. An investigation into CSG water treatment by MED should be considered, as this technology is currently deployed for seawater desalination.

2.4.2 Membrane distillation

Like MED, MD involves the phase change of liquid-water to vapour. Water is retained on a hydrophobic membrane (active layer), while vapour passes through the porous membrane. The process (Figure 7) is driven by a vapour pressure difference, which is influenced by the temperature difference between the *active* (hydrophobic) and the *inactive* membrane surface (Figure 8). The distillate production increases as the temperature difference increases [70, 71]. MD was first discovered by Bodell in 1963, which is yet industrialised (see section 2.5.1) [70, 71].

MD has four configurations. They are: direct contact MD, air gap MD, sweeping gas MD and vacuum MD. None have been successful for large scale applications; however, vacuum and air gap MD being the only configurations used at a pilot scale level [72, 73]. MD is used for many applications such as desalination, pharmaceutical water treatment, juice concentration and heavy metal water removal.

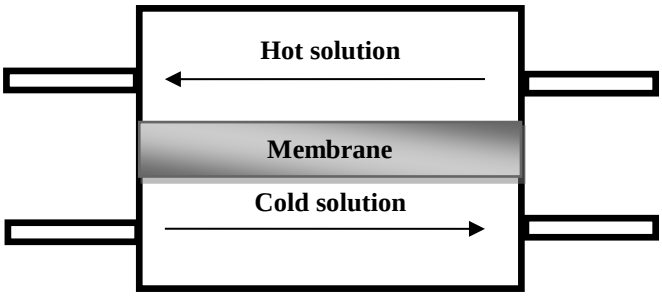

Figure 7: Schematic diagram of a direct contact membrane distillation (DCMD). It is the most used configuration in MD processes (Adapted from [70]).

Membrane thickness is a major characteristic for the membrane process, and is inversely proportional to the mass transfer. Thicker the membrane then lower the distillate productivity [70]. For example, Martinez et al. [74] studied the flux efficiency using two membranes (with identical characteristics) having a membrane thickness of 120 µM and 60 µM. Their results showed the former membrane had an average mass transport of $3x10^{-3}$ kg/m^{2}s, while the latter had an average mass transfer of $6x10^{-3}$ kg/m^{2}s. In another study by Al-Obaidani et al. [60], mass transfer efficiency was observed using membranes with thickness of 250 and 1,150 µm. Their results saw a rapid flux decline of 70% with the thicker membrane. The optimum thickness for MD membranes is between 30 to 60 µm [75].

Mass transfer is proportional to the vapour pressure across the membrane. It is also expressed in the following equation:

$$J = C_m(P_2 - P_3) \qquad \text{Eq. 2}$$

Where C_m is membrane permeability, P_2 and P_3 are the vapour pressure found on feed and distillate surfaces, respectively.

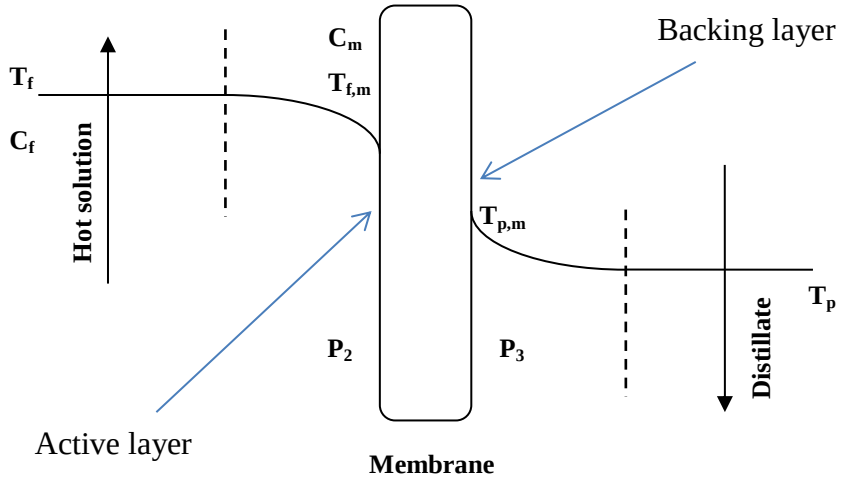

Figure 8: DCMD Mass and heat transfer through hydrophobic membrane process (Adapted from [70]).

For a more concentrated solution, Schofield et al. [76] calculated the rate of mass transfer by the following:

$$J = \frac{dP}{dT}\left[\left(T_{f,m} - T_{p,m}\right) - \Delta T_{th}\right]\left(1 - x_m\right) \qquad \text{Eq. 3}$$

Where ΔT_{th} is assumed temperature threshold and x_m as dissolved membrane fraction within the membrane pores.

Research into CSG water treatment with MD is yet available, although, it is possible for MD to treat CSG RO brine. For example, a study showed 81% of water recovery from RO brine containing 7,500 mg/L of TDS [77]. In another study, RO brine containing 42 g/L of TDS was also treated using MD. The results reported 60% of water recovered from the brine, making it 90% overall from the original source. The rejection of salt was 99.9% [78]. A final study treated seawater brine using a vacuum MD. The TDS content was 50 g/L and the water recovered was 89% [79].

2.5 Industrial application

2.5.1 Membrane distillation

MD is currently not used for large scale production, due to unavailable membrane modules, and high energy demand [71, 72, 75]. Past studies have fabricated synthetic hollow fibre membranes for MD, where the desirable characteristics such as high flux, low liquid entry pressure and heat loss prevention were modified [61, 80]. For instance, a study in 2004 developed and compared a synthetic flat sheet membrane from poly (vinylidene fluoride-co-tetrafluoroethylene) membrane, to poly (vinylidene fluoride) (PVDF) flat-sheets (used for MD). The mechanical properties from the synthetically modified membrane outperformed the membrane prescribed for MD [81]. Another study fabricated a hydrophobic polypropylene hollow fibre membrane, coated with a variety of microporous plasmapolymerized silicone−fluoropolymer. The distillate flow rate was a steady 18 kg/m^2h at 90% water recovery [82]. Though past studies have produced membranes for MD, they are still yet available.

MD was critised for being impractical and too expensive, because of high energy requirement with the distillation process [71]. However, alternative energy sources are available to lower production costs. For example, waste heat or solar driven resources can be substituted for thermal energy. Xu and co-workers used waste heat generated by ship turbines, to raise the temperature of seawater feed to 55°C [73].

2.5.2 Multi-effect distillation

MED is widely used for seawater desalination. Like MD, MED also suffers from high energy demands but meets a lower need in energy requirements, compared to MD [72]. MED is operated in some (or most) cases using solar technology. In the United Arab Emirates (UAE), the first solar powered MED plant was first commissioned in 1983 and operated for 18 years [83]. Today in the UAE, MED distillation plants have a running capacity of 22,700 m^3/day [84]. MED plants can be

found in India's Reliance Refinery, with four MED plants operating since 1998. Each plant has a capacity to produce 12,000 m^3/day. The Refinery has delivered a fifth unit in February, 2005. The unit's capacity is 14,400 m^3/day [85]. The Virgin Islands, USA, has 15 MED plants operating since 1980. A new compact design for the 15 MED plants has reduced capital costs and space, by compacting 3-effects into the one vessel. The capacities of the MED plants are unavailable [85]. China currently has the world's largest MED plant, where production capacity is 200,000 m^3/day. China's MED plant in Tianjin is powered by waste heat generated from the electricity plant. The use of waste heat reduces costs associated to distillation and minimising emissions produced from the electricity plant. China's MED plant also has a zero liquid discharge, where left over brine is recycled and converted into table salt [86]. Al-Shammiri and Safar [63] also reports 18 other commercialised plants.

2.6 Conclusion

The volume and composition of CSG-produced water can vary significantly, depending on the actual geographical setting. However, the CSG industry in Australia is expecting to last for 100 years, and as a consequence, the volume of water will be significant and requiring urgent attention. The decommissioning of evaporation ponds requires CSG operators to look for alternative disposal methods that have minimum environmental impacts. MED is a well-established technology for seawater desalination and could be used to reclaim further water from CSG RO brine. The research gap in this study is post-treatment of RO CSG brine using MED. This application would be feasible in achieving near zero liquid discharge of CSG RO brine. It is hopeful that, minerals and salts from the remaining liquid discharge to be reclaimable. A previous study was successful in recovering NaOH from CSG brine, and others from seawater RO brine. Further investigation into mineral reclamation from CSG RO brine would be ideal, because there is limited literature in this area.

CHAPTER 3: MATERIALS AND METHODOLOGY

3.1 Introduction

This chapter describes the pilot treatment system, experimental procedure and laboratory analyses achieved in the study. The pilot treatment train consisted of an ultrafiltration (UF) pre-treatment, RO, and MED system. The pilot program took place at the Tidemann's property in Gloucester, NSW. Two separate pilot programs were conducted in November 2013 and March 2014, respectively.

3.2 Origin of coal seam gas water

CSG-produced water was collected from the Craven 06 (CR06) and Waukivory 03 (WK03) exploration gas-wells. These exploration wells are located in the Gloucester Basin, Gloucester, NSW (Figure 9). The CSG water is considered in the Upper Permian Gloucester Coal Measures, its age is beyond the limit of the radiocarbon dating method (>30,000 years) and ^{36}Cl dating, points towards several hundred thousands of years. The stable isotopic composition (^{18}O and ^{2}H) indicates both gas-wells to have been caused by meteoric (rainfall) water [26].

CR06 is located 16 km south of Gloucester and drilled from a depth of 983 m below ground level, while WK03, is located 2 km south-east of Gloucester and drilled 818 m below ground level. The specific coal and thicknesses are tabled below[26]:

Table 4: Geology of WK03 and CR06 gas-wells [26].

CR06

Group	Formation	Seam	Top depth	Base depth	Thickness (m)
Gloucester Coal Measures	Crowthers Rd conglomerate				
	Leloma	Bindaboo Coal	149.35	228.09	78.74
		Deards Coal	248.67	358.85	110.18
	Jilleon	Cloverdale Coal	389.74	406.40	16.66
		Roseville Coal	446.96	473.30	26.34
		Tereel Coal	533.22	698.83	165.61
	Wards River Conglomerate		689.86	723.98	25.12
	Wenhams	Bowens Road Coal	723.98	737.9	13.92
	Speldon formation				
	Dogtrap Creek	Glenview Coal	773.61	799.03	25.42
	Waukivory Creek	Avon Coal	852.04	855.70	3.66
		Triple Coal	898.12	917.98	19.86
		Rombo Coal	940.16	950.48	10.32
		Glen Road Coal	954.90	965.63	10.73
	Total		989.00		

WK03

Group	Formation	Seam	Top depth	Base Depth	Thickness (m)
Gloucester Coal Measures	Leloma				
		Roseville Coal	150.31	165.00	14.69
		Tereel Coal	180.68	251.31	70.63
	Speldon Formation				
			304.00	818.00	541.00
	Dogtrap Creek	Glenview Coal	309.72	327.93	18.21
	Waukivory Creek	Avon Coal	434.36	440.72	6.36
		Triple Coal	456.70	481.55	24.85
		Valley View Coal	508.16		
	Total		818.00		

Note: top and base depth is measured in meters below ground level.

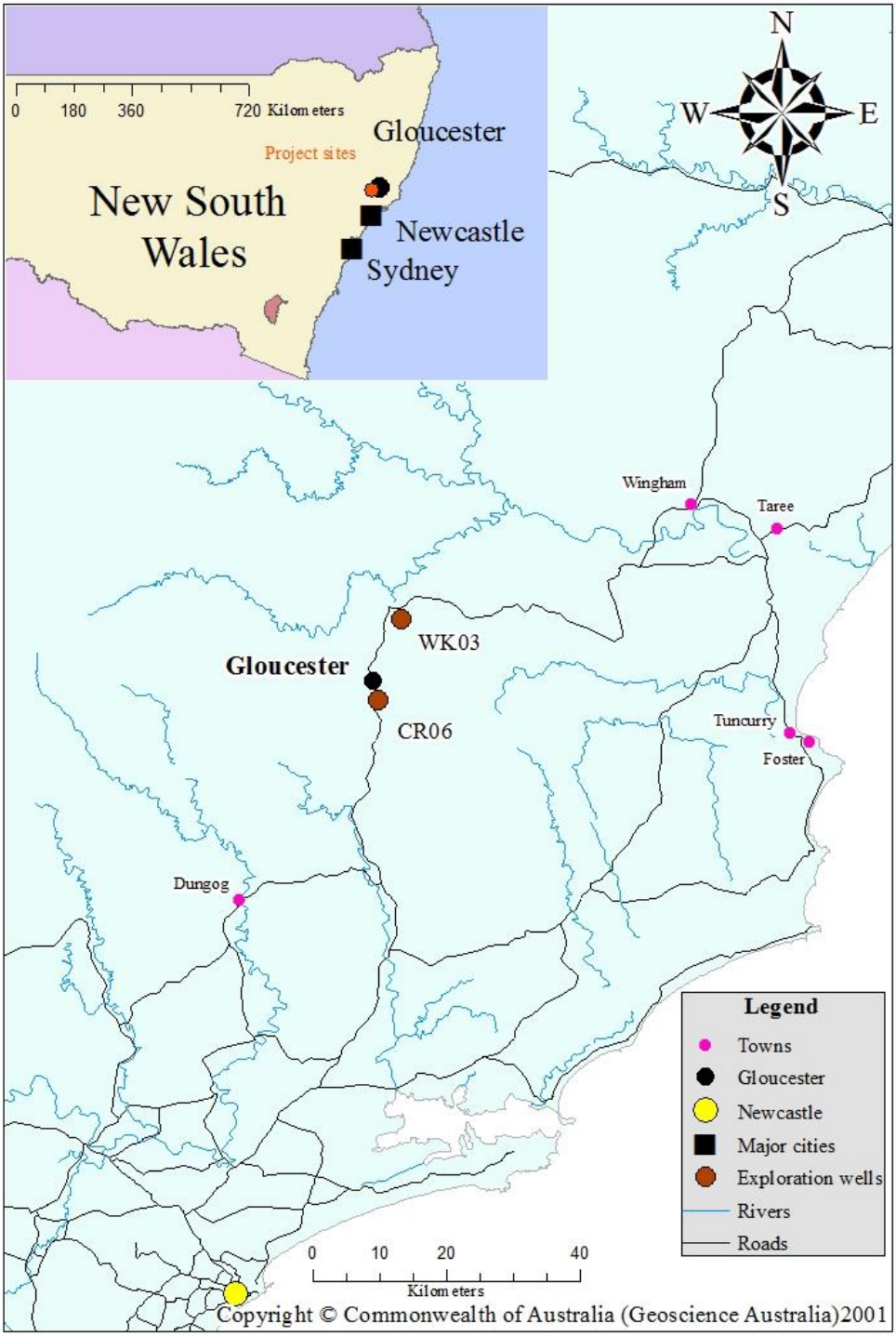

Figure 9: Schematic of AGL's current pilot scale gas exploration for WK03 and CR06, Gloucester, NSW, Australia.

3.3 Site set-up and protocol

The pilot treatment system consisted of a UF pre-treatment coupled with RO and a MED system. CSG water was first pre-treated using UF membranes. Filtrate from the UF was fed to the RO system, producing both permeate and brine. The RO brine was collected and stored in a 1,000 L intermediate container, while the RO permeate (which can be utilised for a range of beneficial use) was discharged to a storage dam. RO brine was treated by the MED system to further extract clean water for beneficial uses. In this study, the MED distillate (clean water) was also discharged to a storage dam, while the MED brine was collected for laboratory analysis and other experiments. A schematic diagram of the pilot treatment train is shown in Figure 10 and a photographic setup in Figure 11. In this study, the MED system was operated continuously throughout the pilot exercise. The UF and RO membranes were only operated during the day, to provide RO brine to feed the continuous MED process. Basic water analysis was taken on-site on a daily basis. Other analyses were conducted in the laboratory at the University of Wollongong (UOW).

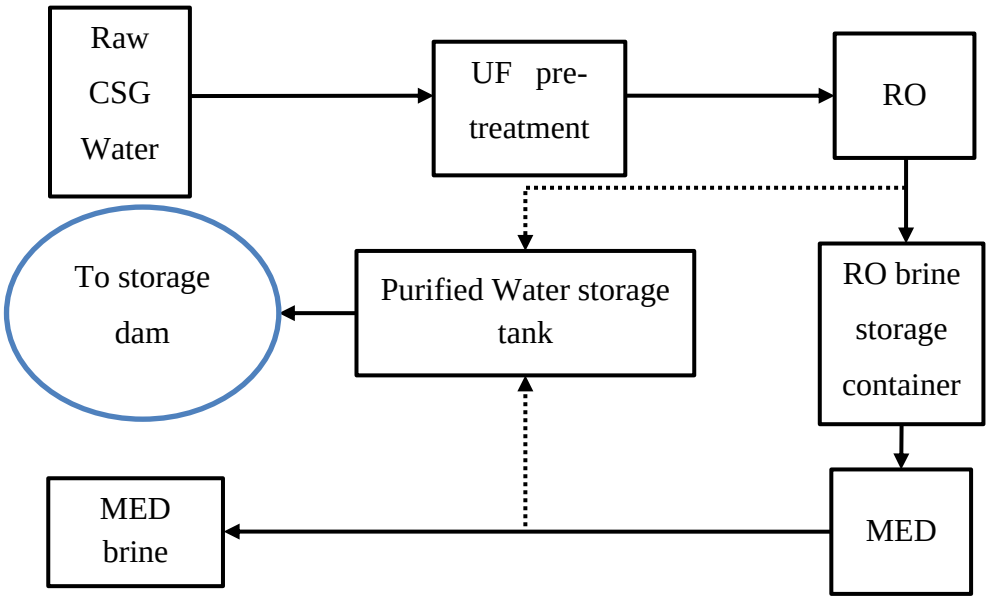

Figure 10: Schematic diagram of CSG water treatment train at AGL's Tiedemann's property, Gloucester, NSW, Australia.

Figure 11: A photograph of the site setup. The following numbered item identifies each component: (1) untreated CSG water storage; (2) UF and RO units; (3) MED unit; (4) cooling tower; (5) cooled water storage, and (6) intermediate storage container (1 of 2) for MED brine storage.

3.3.1 Ultrafiltration/reverse osmosis system

The UF and RO systems were supplied by Osmoflo (SA, Australia). It was housed in a 20 ft shipping container. The UF system consisted of two hollow fibre membrane (hydrophilic polyacrylonitrile (PAN)) modules, with a total active surface area of 48.3 m^2. The membrane average pore size was less than 25 nm. According to the manufacturer, the permeability of this membrane was 93 L/m^2h bar. The UF system was operated on a dead-end mode at 0.55 bar, providing an average flow rate of 2,500 L/h. Each operation cycle consisted of 17 minutes of filtration, followed by 30 seconds of back flushing and 40 seconds of air scouring. The UF system was also equipped with a filter bag to remove any solids greater than 100 µm.

The RO consisted of three brackish membrane modules (AG4040FM, General electrics, Fairfield, CT, USA), which were 4 inches by 40 inches, and an active membrane surface area of 7.9 m^2, each. According to the manufacturer, the membrane nominal NaCl rejection was 99.5%, and the water permeability was 3.09 L/m^2h (at 25 °C and 2 g/L NaCl). The RO system was operated at 17 bar. The water recovery was set at 74%. An anti-scalant (Osmotreat, Osmoflo, SA, Australia) was added to the feed water at 5 mg/L, continuously. Cartridge filters were equipped, (2X20” BB) removing suspended solids greater than 1 µm in size.

3.3.2 Multi-effect distillation

The MED system was supplied by Sasakura Engineering Co., Ltd. (Nishiyodogawa-ku, Osaka, Japan). Two different anti-scalants: Belgard EV2030 (BWA water additives, Tucker, Georgia, USA) and Accent 1131 (DOW chemicals, French Forest, NSW, Australia), were added to the CSG RO brine at 5 and 10 mg/L, respectively. The anti-scalants prevented the precipitation of silica and $CaCO_3$. The MED working temperature was set to 75°C. The vacuum pressure of the evaporation chamber was set to 25 kPa in absolute pressure. The overall water recovery was maintained at specific set points, depending on the actual experiment. Cooling water for the condenser was supplied using an external cooling tower (Aggreko, Wetherill Park, NSW, Australia).

During the March field work, anti-scalants: Belgard EV2030 (BWA water additives, Tucker, Georgia, USA) and Accent 1131 (DOW chemicals, French Forest, NSW, Australia) were replaced with a accelerated precipitation seeding (APS) protocol (Figure 12): magnesium silicate ($MgO•3SiO_2$) and $CaCO_3$ at a dose of 1 g/L, each. The APS was now the new anti-precipitation agent of silica and $CaCO_3$. The RO brine was seeded using an external circulator pump and stored in a separate 1,000 L intermediate tank. The water recovery was set to 88.5% from days one through to four, and later increased to 90% on days five through to nine.

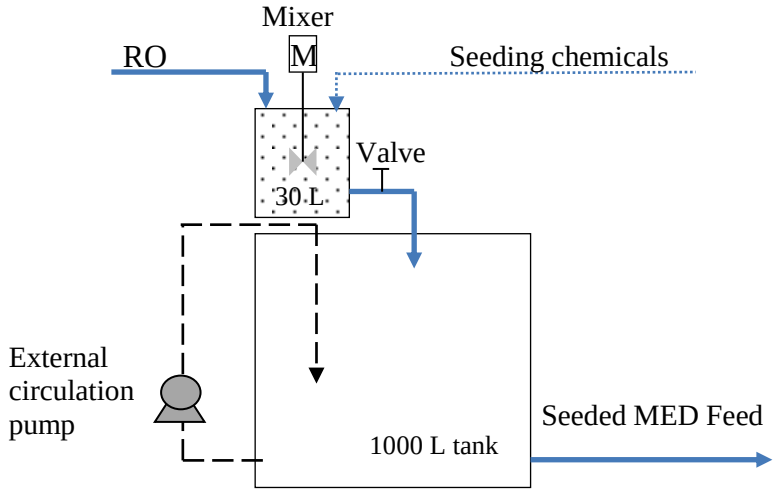

Figure 12: The schematic seeding protocol. Dosage of $MgO•3SiO_2$ and $CaCO_3$ was 1 g/L each per 1,000 L of CSG RO brine.

3.3.3 On-site sample collection and analysis

3.3.3.1 Sample collection

Raw CSG water, UF filtrate, RO permeate, RO brine, MED distillate and MED brine samples were collected on a daily basis. These water samples were collected in 250 mL bottles for analytical analysis at the UOW. Basic water parameters (including pH, conductivity, turbidity, and silica concentration) were measured on-site as described below.

3.3.4 Sample analysis

Basic water parameters such as pH, conductivity, turbidity and silica concentrations were measured immediately upon sample collection. These measurements were conducted daily for the duration of field work. These measurements were conducted as they have a strong influence on performance of the pilot system. High silt and turbidity levels will foul the membrane, which effectively reduces permeate production. pH is important to monitor and prevent the solubility of silica, which can cause membrane scaling and, conductivity, is a strong measure for salt removal and permeate quality.

The pH and conductivity measurements were logged, using an Orion 4-Star Plus pH/conductivity meter (Thermo Fisher Scientific, Waltham, MA, USA) (Figure 13). Firstly, a beaker was cleaned using MED distillate and then filled with the sample. The pH/conductivity probes were rinsed and submerged into the beaker for a complete measurement.

Figure 13: The Orion 4-Star Plus pH/conductivity meter used in this study.

Turbidity analysis was conducted using a HACH 2100Qis portable turbidity meter (Hach, CO, USA) (Figure 14). Vials were firstly rinsed three times with distillate and once with the sample. The vial was filled with the sample and then cleansed using a silica gel agent, removing impurities intact on the glass surface. This allowed for minimum interference during the measurement.

Figure 14: Portable Hach 2100Qis turbidity meter.

Silica analysis was executed using a pocket colorimeter II (Hach, Colorado, USA) (Figure 15). Firstly, the sample cell was rinsed and filled with distillate for calibration; afterwards, 10 mL of sample filled the cell. In each sample cell, molybdate reagent and acid reagent powder pillows (Hach Pacific-Australia) were supplemented. This step increased the silica range showing the presence of silica, when an intense yellow colour was formed. After 10 minutes, a sachet of citric acid (Hach Pacific-Australia) was added, to destroy traces of phosphorus interfering with the analysis. After a 2 minutes period, the citric acid reaction was complete and concentration of silica was recoded in mg/L.

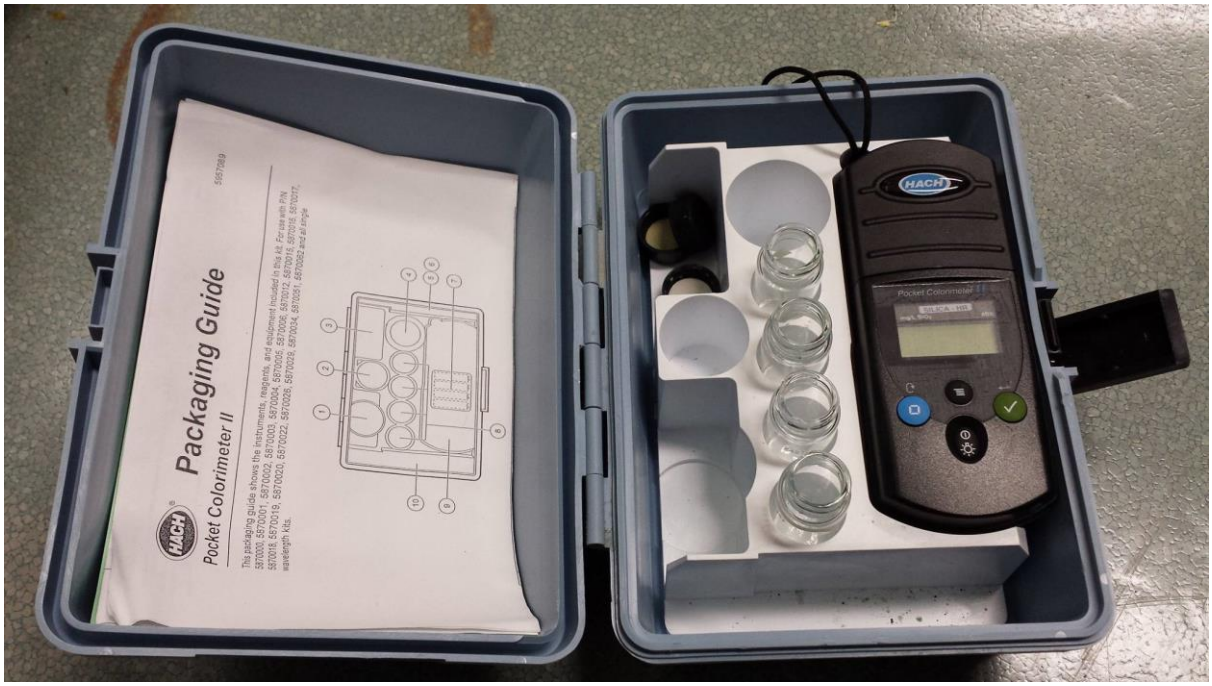

Figure 15: Pocket colorimeter II (Hach) for silica analysis.

3.4 Laboratory analysis

Laboratory analysis was conducted on the CSG-produced water sampled from Gloucester. This was integral for the thesis, as it provided results that could not be collected on field. Measurements such as organic carbon, specific cations and anions were run through instruments (described below) to determine the total removal of specific constituents, commonly found in Australian CSG-produced waters.

3.4.1 Total organic carbon, total carbon and bicarbonate

Total organic carbon (TOC) and total carbon (TC) were analysed using a Shimadzu TOC/TN-V_{CSH} analyser (Shimadzu, Japan, Kyoto) (Figure 16); the mode setting was set to non-purgeable organic carbon (NPOC). For TOC: raw CSG water, UF-filtrate, RO permeate and MED distillate were placed into the analyser with the exception of RO and MED brine, diluted a 100 times before analysis. Samples were removed and then measured for TC. TC samples were acidified below pH 2 with 4 mol/L HCl. This screened for interferences (i.e. inorganic carbon) and was left to aerate for 5 minutes; a complete reaction time was indicated by the presence of fumes. All

samples were measured against calibrated solutions from 0 to 100 mg/L. Concentration of TC and TOC were given in mg/L. Bicarbonate content was calculated subtracting TC from TOC.

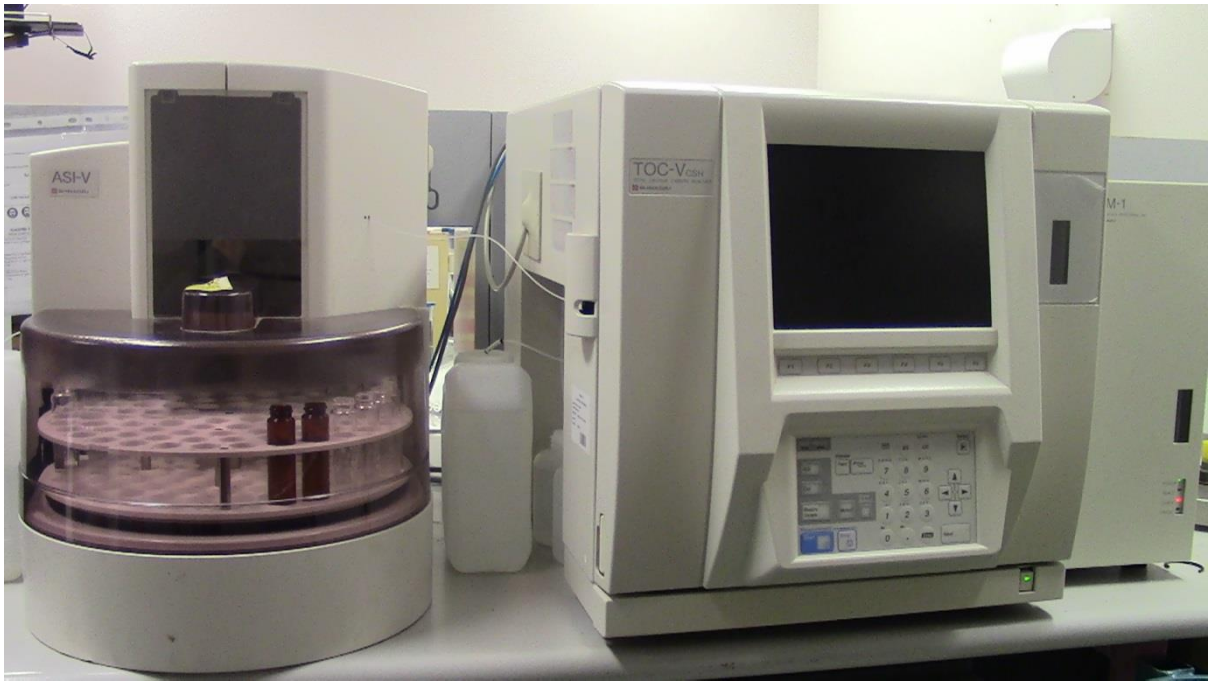

Figure 16: The Shimadzu TOC/TN-V_{CSH} analyser for TOC and TC measurements.

3.4.2 Anion analysis

A LC-20AC Ion Chromatography (IC) system (Shimadzu, Kyoto, Japan) (Figure 17) was used to measure the concentration of Cl^-, SO_4^{2-} and NO_3^-. The IC system was equipped with a Dionex Ion Pac AS23 anion exchange column (Thermo Scientific, Waltham, Massachusetts, USA), which measured the anionic interaction of Cl^-, SO_4^{2-} and NO_3^- found in the RO and MED brine. Calibrated standards of each anion were made up to 5, 10, 50 and 100 mg/L. The eluents Na_2CO_3 and $NaHCO_3$ had a concentration of 4.5 and 0.8 mmol/L, respectively, and an average flow rate of 1 mL/minute. The injection volume for all standards and samples were 10 µL.

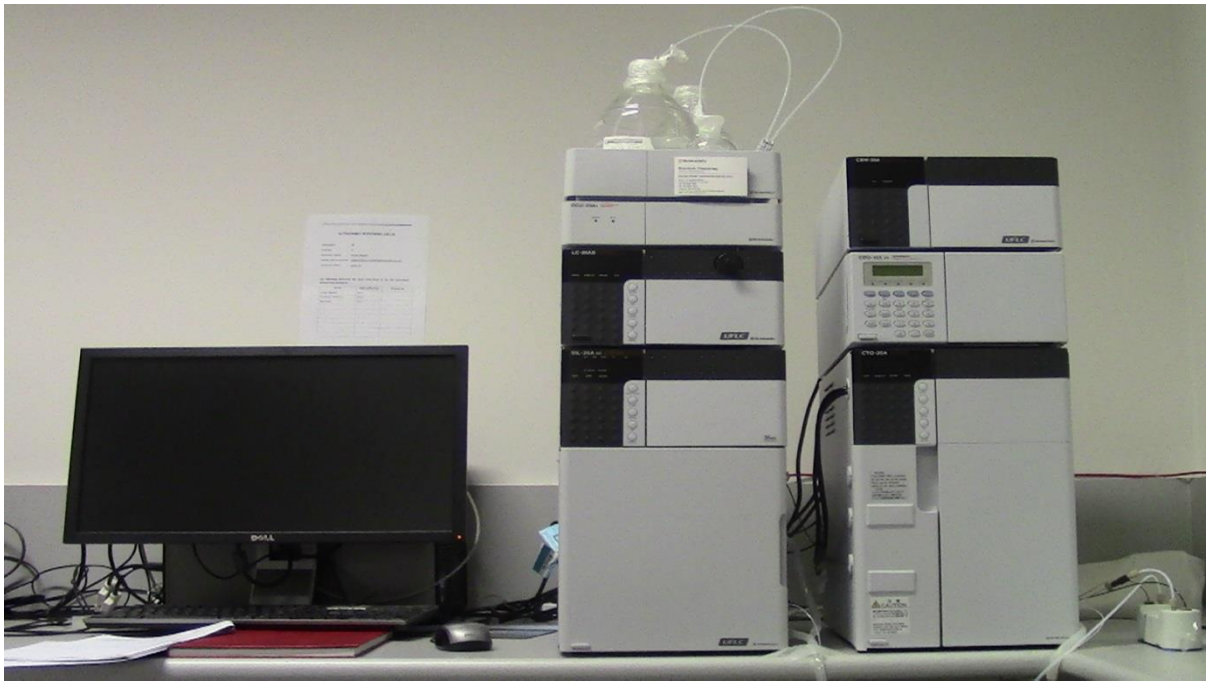

Figure 17: The IC system used in this study.

3.4.3 Cation analysis

Cations including Mn^{2+}, Al^{3+}, Na^{2+}, K^{+}, Mg^{2+}, Ca^{2+} and Fe^{3+}/Fe^{2+} were separated using a Agilent 7500 CS (Agilent Technologies, Wilmington, DE, USA) inductively-coupled plasma mass spectrometer (ICP-MS) (Figure 18). The CSG water samples were prepared with 2% nitric acid and diluted 2,000 fold. Standard solutions were prepared according to the manufacture manual from 0 to 500 µg/L. The Injection volume for both standard and sample solutions was 5 mL. The injection of CSG water aliquot samples were performed three times for each batch, measuring the average and accurate mass to charge ratio (m/z).

Figure 18: The ICP-MS system used in this study.

A high frequency 3MHz mass quadrapole was used to filter cations to their m/z. Contamination throughout the procedure was avoided by disinfecting apparatuses with 5% nitric acid. The calibration of ICP-MS was performed at the start of each batch samples, using a multi-element tuning solution made up of 10 µg/L of Li, Y, Ce, Tl and Co. The ICP-MS was injected with 5 mL of standard solution every five samples, to analyse the performance of the instrument. Calibration curves for each separation method were generated at the end with a $R^2 > 0.99$, and later converted into mg/L.

3.4.4 Ultrafiltration fouling potential analysis

The silt density index (SDI) measured the fouling potential of CSG water on the UF membranes. This parameter is important in designing a pre-treatment system for a worse-case scenario. The SDI was calculated by the following equation:

$$SDI_{15} = \left(\frac{1 - \frac{t_i}{t_f}}{15} \right) 100 \qquad \text{Eq. 4}$$

where t_i is the initial time in filtering 500 mL of water and t_f requiring the final time to filter 500 mL of water 15 minutes after the experiment. The laboratory set-up (Figure 19) measured the plugging potential of a nitrocellulose white disk (HAWP04700, Millipore, Australia) operated at 2 bar of constant pressure. The pore size, diameter and surface area of the membrane disk was 0.45 µm, 47 mm and 1.73×10^{-3} m^2, respectively. The SDI values for raw and UF filtrated CSG-produced water were evaluated in this work. A photo of the SDI apparatus is shown in Figure 20.

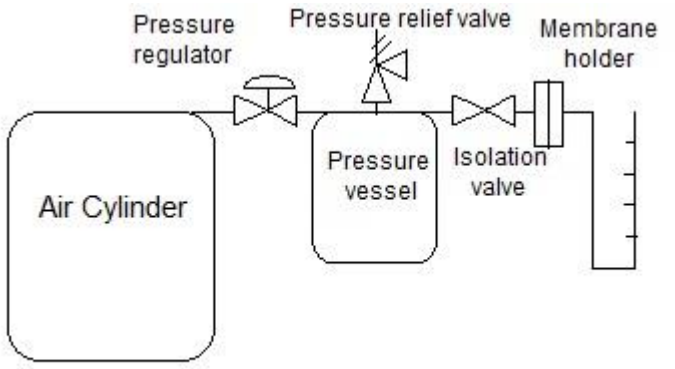

Figure 19: A schematic of the SDI apparatus.

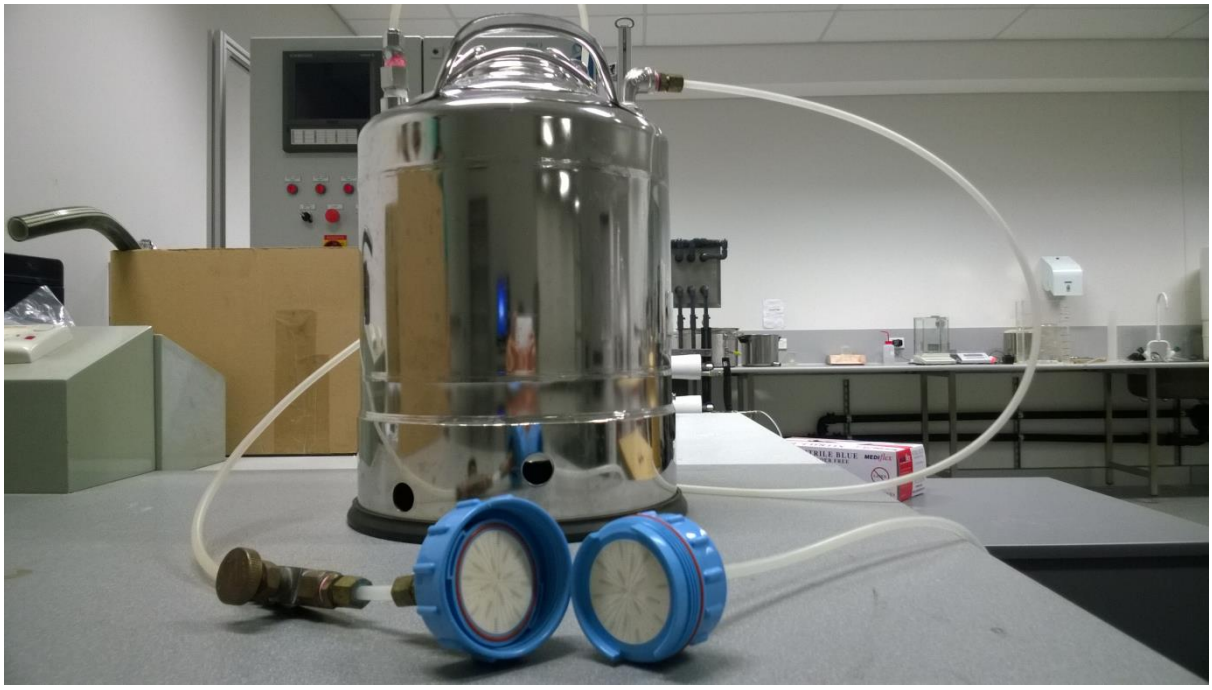

Figure 20: Laboratory scale SDI apparatus.

CHAPTER 4: RESULTS AND DISCUSSION

4.1 Waukivory and Craven gas-well water characteristics

In Australia, CSG-produced water is mostly brackish. The characteristics for WK03 and CR06 produced waters are shown in Table 5. As expected, WK03 and CR06 gas-wells are slightly brackish (Table 5). The salinity of CSG-produced water is influenced by organic material forming the coal deposits. Thus, coal deposits can be associated with either brackish or marine like waters, depending on the quality of coal formed and its grade [87].

TDS in CR06 was 1.4 times greater than WK03. The ionic composition for both WK03 and CR06 gas-wells is dominated by Na^+, Cl^- and HCO_3^-. These three constituents compose 87 and 95% of WK03 and CR06, respectively. Previous studies have also shown these ionic properties to dominate CSG-produced water from other gas fields, and make up as the main constituents in the natural gas waters [19, 23, 88-91]. Concentrations of Cl^- were also greater in CR06 CSG-produced water than WK03 (Table 5). According to Van Voast [19], Cl^- concentration can vary, depending on the hydrological setting. For example, concentrations of Cl^- may be lower for WK03 because of a nearby recharge area. It is noteworthy that CR06 and WK03 gas-wells were selected for investigation because they present the highest and lowest salinity level, respectively, from Gloucester's gas fields.

Concentrations of Ca^{2+} were 24.98 and 9.68 mg/L for WK03 and CR06, respectively. Ca^{2+} was higher for WK03 than CR06, because of the depth of the coal seam. WK03 produced water was extracted 818 m below the surface, whereas CR06 was extracted 983 m below the surface. Produced waters in deeper strata have depleted Ca^{2+} than those from shallower waters [88]. Mg^{2+} showed no difference in concentration levels between WK03 and CR06. The concentrations of Mg^{2+} and Ca^{2+} in comparison to the other major ions are low. High levels of HCO_3^- depletes Mg^{2+} and Ca^{2+} ions from soil profiles [19]. Thus, both Mg^{2+} and Ca^{2+} can react with CO_3^{2-} to precipitate as dolomite and calcite. Concentrations of Fe^{3+}/Fe^{2+}, K^+ and Al^{3+} were marginally higher in WK03 than CR06 produced waters (Table 5).

Table 5: Characteristics of CSG produced water from the WK03 and CR06 gas-wells.

Parameters	WK03	CR06
TDS (g/L)	2.51	3.57
Turbidity (NTU)	32	6.1
TC (mg/L)	337	395
TOC (mg/L)	1.69	29
HCO_3^- (mg/L)	1711	1916
SDI (-)	6.3	6.3
Na^+ (mg/L)	1351.24	1770
Cl^- (mg/L)	62.19	1404
Mg^{2+} (mg/L)	4.79	4.8
Al^{3+} (mg/L)	7.53	0.01
K^+ (mg/L)	29.06	8.19
Ca^{2+} (mg/L)	26.48	27.9
Mn^{2+} (mg/L)	0.08	0.1
Fe^{3+}/Fe^{2+} (mg/L)	43.57	58.67
Silica (mg/L)	18	19

The sodium adsorption ratio (SAR) and conductivity for WK03 and CR06 CSG-produced waters is presented in Table 6.

Table 6: SAR, pH and conductivity of raw CSG produced water.

Gas-well	SAR (meq/L)	pH (-)	Conductivity (mS/cm)
WK03	63.5	8.4	4.45
CR06	81.3	8.2	6.55

The SAR and electrical conductivity (Table 6) can be used together to assess the suitability of CSG-produced water for irrigation. As illustrated in Figure 21, irrigation using water with low SAR and low electrical conductivity may result in long term soil degradation, by reducing the infiltration capacity of a soil profile. The electrical conductivity and SAR for WK03 and CR06 was 4.5 and 6.5 mS/cm, and 63.5 and 81.3 meq/L, respectively. Both WK03 and CR06 would cause significant

soil infiltration reduction, if used directly for irrigation purposes or discharged as waste into environmental systems (Figure 21).

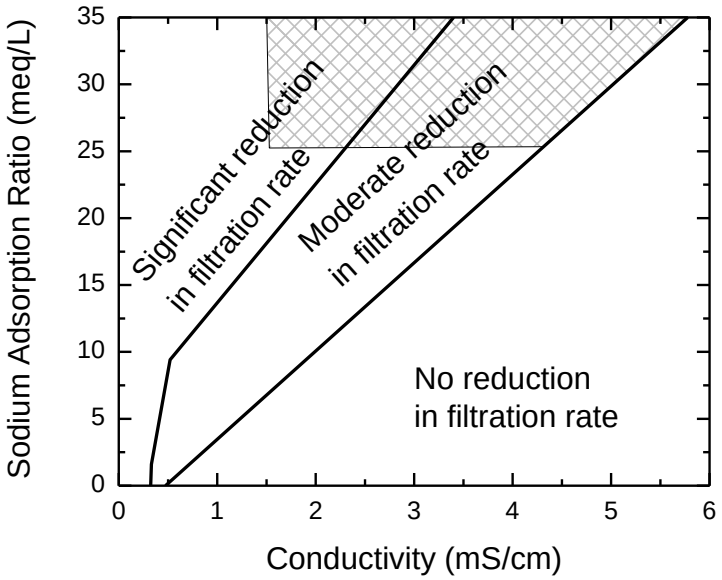

Figure 21: The relationship of SAR vs electrical conductivity (from [3]).

The pH (Table 6) was 8.37 and 8.2, respectively, for WK03 and CR06, which is slightly alkaline. Water alkalinity is a result of CO_2 degassing, when exposed to atmospheric conditions (typically when stored in evaporation ponds) [22, 23]. However, WK03 and CR06 gas-wells were not stored in evaporation ponds, but in confined shipping containers, thus, no evidence of degassing of CO_2 by atmospheric conditions.

4.2 Comparison between Gloucester and Bowen Basins

WK03 and CR06 were compared to three (from 79 surrounding Glenden, Moranbah, Dysart and Middlemount) gas-wells from Bowen Basin, QLD [92]. Parameters such as TDS, pH, conductivity and common ions were measured and are presented in Table 7.

Table 7: Chemical characteristics from 3 gas-wells in Bowen Basin, QLD, Australia.

Parameters	GM1V	GM014V	GM015V
pH (-)	7.38	7.79	7.45
EC (mS/cm)	11.04	9.030	9.260
TDS (g/L)	6.796	5.696	5.826
TOC (mg/L)	20	167	85
HCO_3^- (mg/L)	519	1480	1640
Na^+ (mg/L)	2270	1960	2120
Cl^- (mg/L)	3679	2397	2373
Mg^{2+} (mg/L)	55	9	12
Al^{3+} (mg/L)	<0.01	<0.01	<0.01
K^+ (mg/L)	46	10	12
Ca^{2+} (mg/L)	76	20	22
Mn^{2+} (mg/L)	0.02	<0.01	0.02
Fe^{3+}/Fe^{2+} (mg/L)	0.06	0.21	<0.01
Silica (mg/L)	8.65	9.29	10.1

Ionic substances in Bowen Basins GM1V, GM014V and GM015V gas-wells are dominated by Na^+ and Cl^- and HCO_3^- (Table 7). These are also the three major constituents in WK03 and CR06.

The pH for Bowen Basin exhibits alkaline conditions similar to Gloucester's gas-wells. However, pH was below 8 for Bowen Basin, whereas WK03 and CR06 pH was above 8. Higher pH in Gloucester's gas-wells is associated to intense weathering of CO_3^{2-} (associated with HCO_3^-), because concentrations of HCO_3^- are higher compared to the three Bowen Basin gas-wells. Alkalinity is associated with weathered minerals [93].

Silica is accumulated by weathered Basalt. Gloucester and Bowen Basin both have Basalt overlain rocks, and on average, silica is two times greater in Gloucester compared to Bowen Basin gas-wells. Silica for Bowen Basins GM1V, GM014V and GM015V are 8.65, 0.29 and 10.1 mg/L, respectively.

Fe^{3+}/Fe^{2+} in Bowen Basin are almost negligible compared to Gloucester's gas-wells, while TOC are higher in Bowen Basin gas-wells. The increased levels of Fe^{3+}/Fe^{2+} and TOC is a result of igneous rock formations susceptible to weathering and dissolution of ion [26, 93].

SAR is more concerning in Bowen Basin than Gloucester's gas-wells. SAR is higher in Bowen Basin, because of higher Na^{+} and electrical conductivity compared to Gloucester's gas-wells. The SAR for Bowen Basin's three gas-wells is given in Table 8. However, both Gloucester and Bowen Basin gas-wells are high in Na^{+} and low in Ca^{2+} and Mg^{2+} exchangeable ions, with a high sodium-associated electrical conductivity. SAR for GM1V is lower compared to WK03 and CR06 gas-wells, because of higher levels of HCO_3^{-} due to weathering processes. [92]. Produced waters from the three Bowen Basins pose a greater risk to ecology than the Gloucester gas fields.

Table 8: SAR of CSG produced water from the Bowen Basin.

Water source	SAR (meq/L)
GM1V	48.4
GM014V	91.4
GM015V	90.3

4.3 Performance of pilot train

4.3.1 Membrane processes

The performance of UF and RO membranes will be discussed here, with respect to water flux and permeate quality. Overall, the permeate flux for both the UF and RO membranes was stable. Higher RO recovery was obtained from WK03 gas-well than CR06. The UF water flux averaged 50 L/m^2h for both WK03 and CR06 gas-well.

4.3.1.1 Ultrafiltration performance stability and permeate quality

The purpose of UF pre-treatment is to operate the RO system in safe and stable conditions, and to provide good quality water. The UF performance of WK03 and CR06 is exhibited in Figure 22. Figure 22 shows a stable performance for UF operation. The trans-membrane pressure was also fixed at 0.55 and 0.24 bar, respectively. Higher trans-membrane pressure alters water quality and water flux performance; the overall flux for WK03 and CR06 confirms this. The average UF flux for WK03 was 52.6 L/m^{2}h, and 48.8 L/m^{2}h for CR06. Chemical cleaning and scourging of UF membranes effectively restored the water flux.

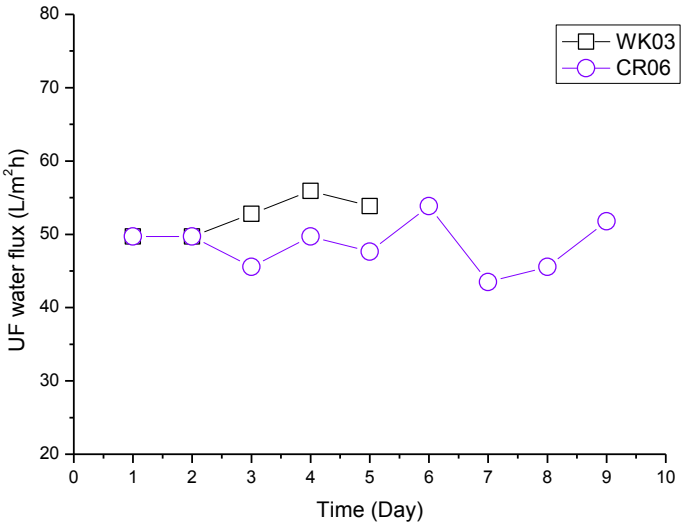

Figure 22: Water flux as a function of time: WK03 and CR06 (hydrophobic-PAN module, operating pressure = 0.55 and 0.24 bar, respectively, membrane back flushing every 17 minutes (membrane characteristics see 3.3.1)).

Both WK03 and CR06 gas-wells have high levels of particulate matter, which could critically impair the RO membranes and limit its performance. The high level of particulate matter is reflected of high turbidity and SDI. It is noted that UF filtration did not change the characteristics of the CSG-produced water, other than turbidity and SDI. This is expected as the pore size in UF is manufactured to retain only particulate matter but not dissolved substances. Turbidity of the raw CSG-produced water was high as can be seen in Table 5. The removal of turbidity was higher in WK03 than CR06. However, the UF filtrate for both WK03 and CR06 produced

waters was less than 0.6 NTU (Figure 23). The high rejection of particulate matter was effective and able to meet the operating conditions for RO [94]. The turbidity removal was greater than 98 and 96% for WK03 and CR06 CSG-produced waters, respectively.

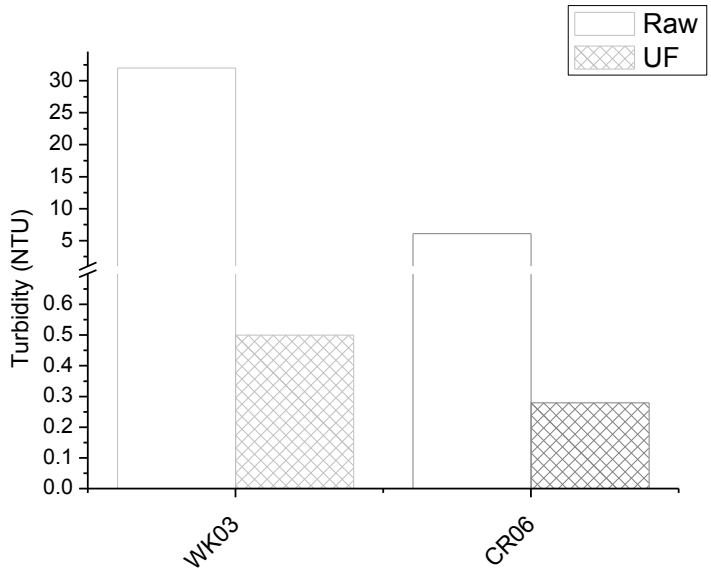

Figure 23: Rejection of turbid pollutants using UF membranes.

SDI is an empirical parameter and is a surrogate measure for fouling potential by particulate feed water. Particulate and colloidal pollutants influence the SDI value and whether SDI pre-treatment is required. SDI for untreated WK03 and CR06 CSG-produced waters (Table 5) is 6.3, each. The performance of the UF pre-treatment is illustrated in Figure 24.

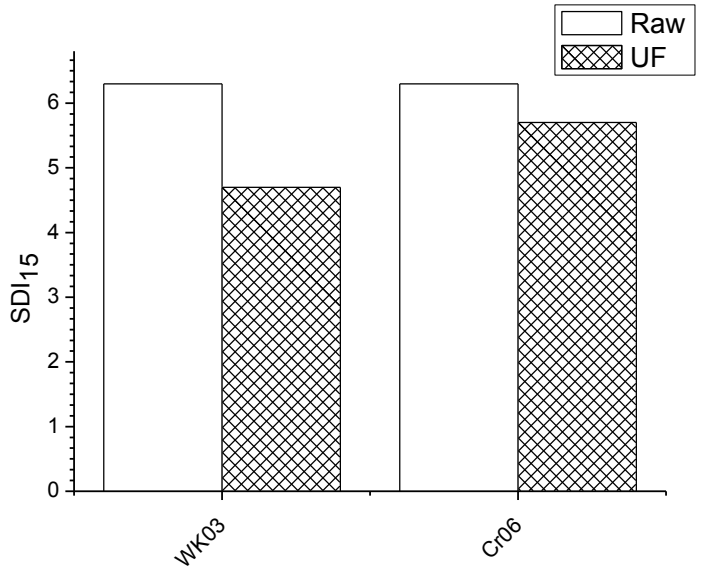

Figure 24: SDI_{15} of untreated and pre-treated CSG-produced waters (applied pressure = 2 bar, nitrocellulose white disk (see 3.4.4 for characteristics)).

After pre-treating WK03 and CR06, the SDI was 4.8 and 5.7, respectively. The essential SDI for RO feed water is 5 and below. The SDI for CR06 UF-filtrate was 0.7 above RO operating guidelines, while WK03 was within 0.2 (Figure 24). Though SDI for CR06 UF-filtrate was above the RO operating conditions, the RO membranes remained stable in its entire operation and were not impaired (see section 4.3.1.2.1). The fouling potential indicates a relation to non-particulate matter, and not associated by SDI. Particles below the nominal pore size of the membrane is responsible for the measure of SDI [95]. Total reduction in SDI for WK03 and CR06 was 25.4 and 9.5%, respectively.

4.3.1.2 Performance of reverse osmosis membranes

4.3.1.2.1 Process stability

Figure 25 shows a stable RO system, with no evidence of fouled membranes. Permeate recovery was 76 and 74% (17 bar of pressure), respectively, for WK03 and CR06. The TDS of UF filtrates influenced the permeate recovery (2% difference).

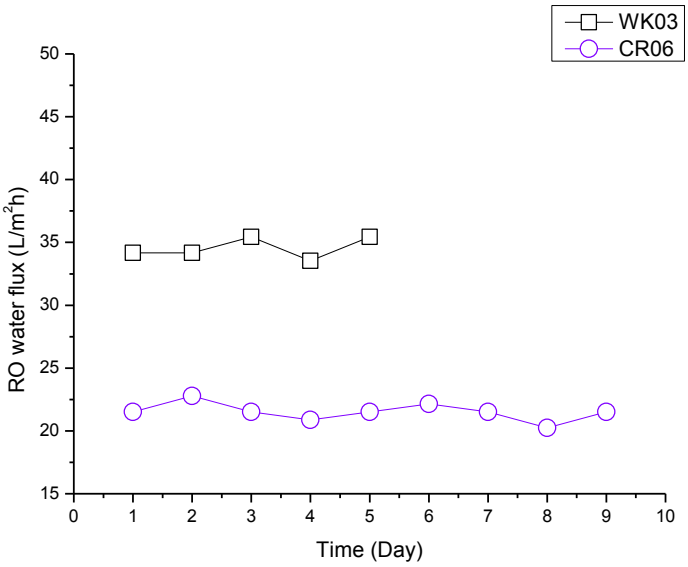

Figure 25: Water flux as a function of time: WK03 and CR06 (AG4040FM membrane, operating pressure = 17 bar, dosage of anti-scalant = 5 mg/L). Membrane characteristics see 3.3.1.

In Figure 25, permeate flux is greater for WK03 than CR06, with respective flow rates of 34 and 22 L/m^{2}h. The salt content was greater in CR06, and would have required higher applied pressure if permeate flux was to remain equal for both experiments [96].

4.3.1.2.2 Permeate characteristics

Permeate characteristics for WK03 and CR06 are shown in Table 9 and Table 10 respectively. The rejection of ionic solids were between 93 to 100%.

Table 9: Concentration (mg/L) of ionic solids for WK03 during RO process.

	Na	Cl	Mg	Al	K	Ca	Mn	Fe
RAW	1351.24	62.19	4.79	7.53	29.06	26.48	0.08	43.57
UF filtrate	1225.2	64.87	4.2	8.48	15.32	28.7	0.13	88.47
RO conc.	4449.84	186.48	12.87	13.76	38.99	40.31	0.13	144.3
RO perm.	6.87	0.24	0.07	0.03	1.31	0.86	0	2.39
R (%)	99.49	99.61	98.54	99.6	95.49	96.75	100	94.51

Table 10: Concentration (mg/L) of ionic solids for CR06 during RO process.

	Na	Cl	Mg	Al	K	Ca	Fe	Si
RAW	1770	1404	5	0	8	10	0	13
UF filtrate	1779	1265.33	4.67	0	8.67	10.67	0.67	14
RO conc.	6842	5604	17.67	0	33	13.67	3	68.33
RO perm.	18	13.67	0	0	0	0.67	0	0.67
R (%)	99.9	99.03	100	100	100	93.3	100	94.85

The rejection of salt (conductivity) for WK03 and CR06 is greater than 99% (Figure 26a and Figure 26b). The conductivity was 4.4 and 6.6 mS/cm, respectively, and less than 0.1 mS/cm in the permeate. The permeate conductivity was lower for WK03 than CR06, because it was more dilute (76% recovery). The conductivity of the brine was 15.0 and 21.9 mS/cm, which is an increase of 71 and 70% from the original water source.

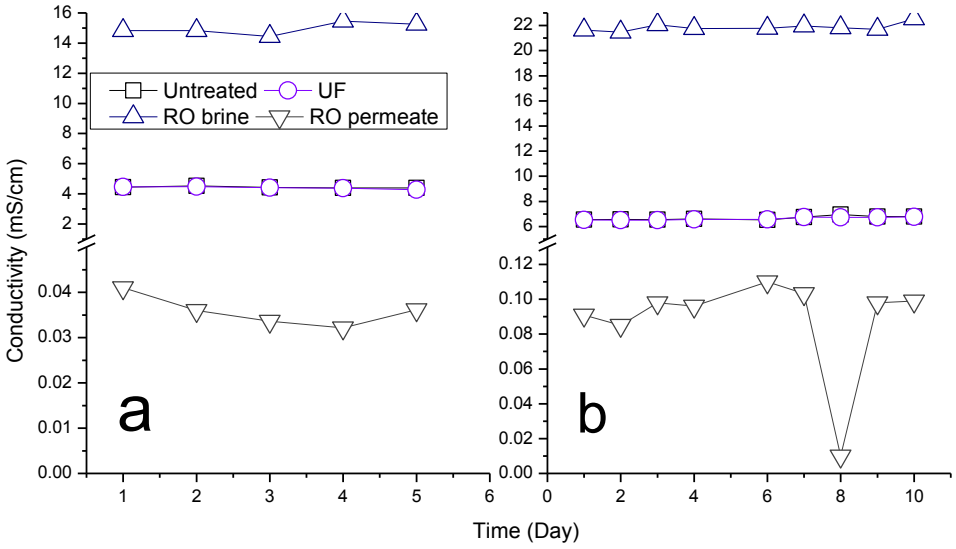

Figure 26: Conductivity as a function of time: (a) WK03 and (b) CR06.

The pH for the membrane process is given in Figure 27a and Figure 27b. The pH showed no change for untreated CSG-produced waters, UF filtrate and RO brine; whereas fluctuation was more obviously in the RO permeate. On average, the permeate pH were subsequently 8.37, 8.43, 8.34 and 6.47 for WK03, and 8.16, 8.21, 8.13 and 6.65 for CR06. Figure 27a and Figure 27b shows pH decreasing in the

permeate and increasing in the brine. Permeate pH decreases because dissolved gases entering the permeate reacts with water, to form the following:

$$CO_2 + H_2O \rightarrow HCO_3 + H^+$$

The adsorption of CO_2 will shift the solution pH to an acidic nature, thus establishing new carbonate equilibrium. The brine pH increases because hydrogen ions are lower and degassing of CO_2 when exposed to atmospheric conditions. This trend is consistent with other research [97, 98]. The pH variation for WK03 and CR06 is negligible.

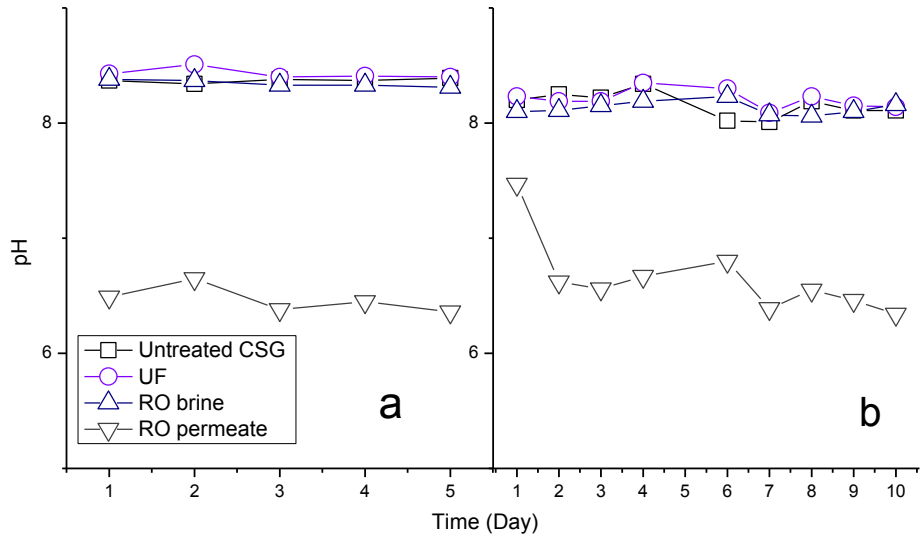

Figure 27: pH as a function of time: (a) WK03 and (b) CR06.

The turbidity in WK03 is relatively similar to CR06 permeate (Figure 28a and Figure 28b). Turbidity was below 0.1 NTU except once for WK03; while three times did the turbidity exceeded 0.1 for CR06 permeate. The turbidity for both WK03 and CR06 permeates is of high quality and good enough to pass as drinking water standards.

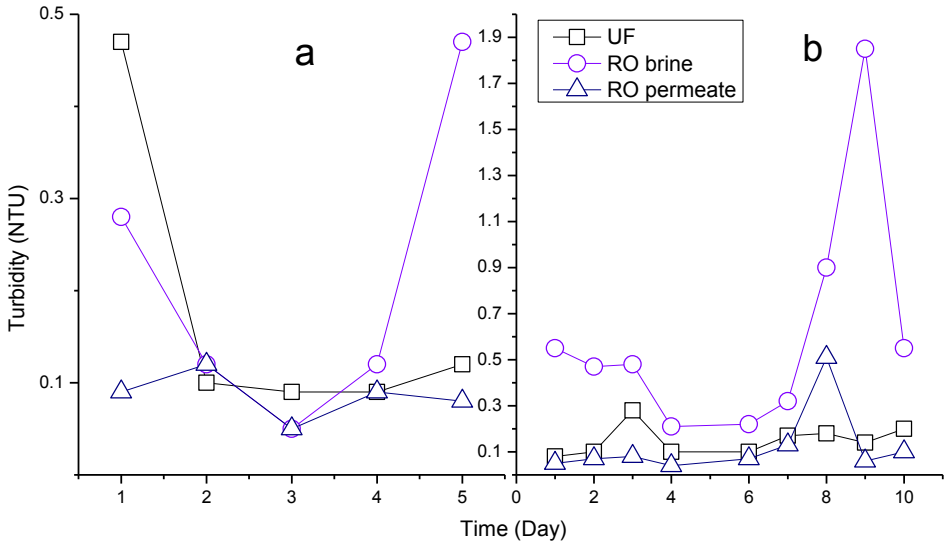

Figure 28: Turbidity as a function of time: (a) WK03 and (b) CR06.

4.3.1.2.3 Brine

All ionic solids increased proportional with water recovery, except for Ca^{2+} and K^{+}. The proportion of Ca^{2+} to water recoveries was 34 and 22% for WK03 and CR06 brine, respectively. Ca^{2+} ions may have retained on the RO membranes, which explains the disproportionate increase of the RO concentrates. However, scaling was not observed on the membranes, but may cause scaling on the membrane surface over long term operation. While silica was not measured in WK03, proportional increase was noted in CR06. The presence of silica does impair the RO process, but is often triggered or catalysed by other ions (i.e. Fe^{2+}/Fe^{3+} and Al^{3+}) [99-102]. In CR06 Fe^{2+}/Fe^{3+} and Al^{3+} were not detected, which may have influenced a proportional increase in RO brine of silica, preventing scaling to occur. However, Al^{3+} and Fe^{2+}/Fe^{3+} did exist in WK03, but showed no evidence of scaling because of silica. This may also be a problem in the long run. A TDS analysis was conducted by evaporating 20 mL of untreated and processed CSG water at 100°C. The TDS in the permeates was as low as 0.13 g/L, while WK03 and CR06 CSG brines were 10 and 14 g/L (Figure 29).

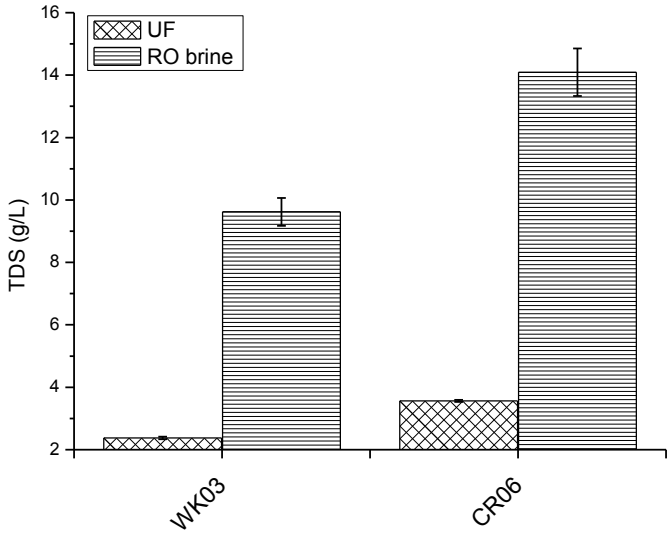

Figure 29: Illustrates the TDS in UF and RO brine.

TDS in WK03 and CR06 brine was approximately 75% of its original source. TDS rejection for permeate WK03 and CR06 was 94.4 and 96.6%.

4.3.2 Multi-effect distillation

The MED pilot experiments are discussed here and addressing the high distillate recovery as its primary function. The quantity of RO brines treated by the MED system is shown in Figure 30a and Figure 30b. A total of 3,002 and 3,176 L of WK03 and CR06 RO brine, respectively, was treated, which contained 22.03 and 109.29 g/L of NaCl salts. Overall, the daily distillate production was steady, as seen in the proportional increase of distillate and retentate illustrated in Figure 30a and Figure 30b. Production of high-quality distillate was successful, and is discussed further in this section. In general, the MED system is a practical tool for treating CSG-produced waters. The distillate produced from WK03 and CR06 RO brine was 2,311 and 2,760 L, while MED brine was 612 and 354 L.

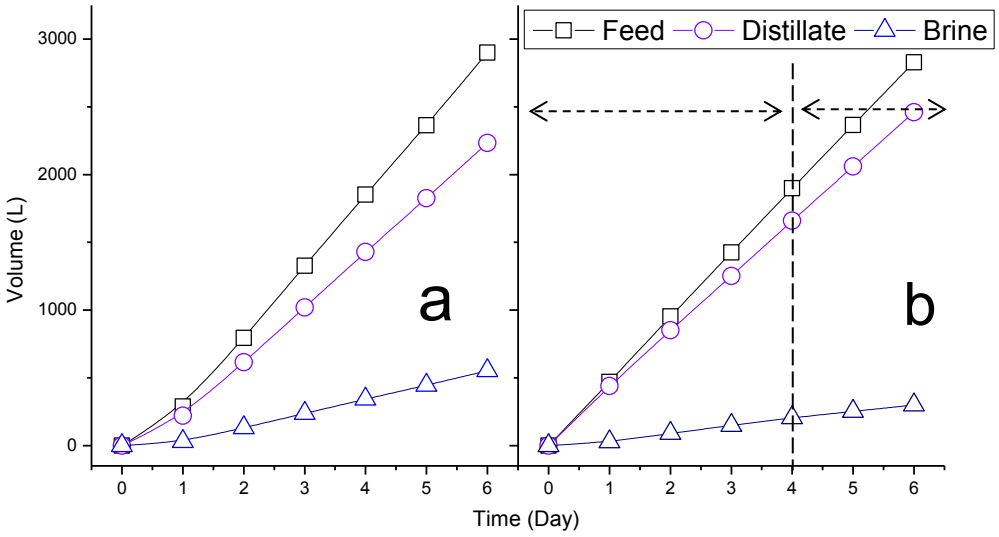

Figure 30: This figure illustrates the volume of RO brine treated with MED and its products (distillate and brine) as a function of time: (a) WK03 and (b) CR06.

4.3.2.1 Process stability

The MED processing WK03 and CR06 RO brines (Figure 31a and Figure 31b), were overall good. The MED produced on average, 16 to 17 L/h of distillate, and a daily production of 0.38 to 0.41 m^3/day. In Figure 31a, the distillate shows no decline in production for WK03, whereas, CR06 (Figure 31b) was less stable, and began to decline in the later part of the experiment. The WK03 experiment did not change, while CR06 did from eight to 10 times of the concentration ratio. The concentration ratio increase in CR06 occurred on day four of the experiment, which is when the declining distillate was observed. This increase would have influenced precipitation of divalent ions, thus reducing the flow rate [103]. The processing performance of the MED was generally good.

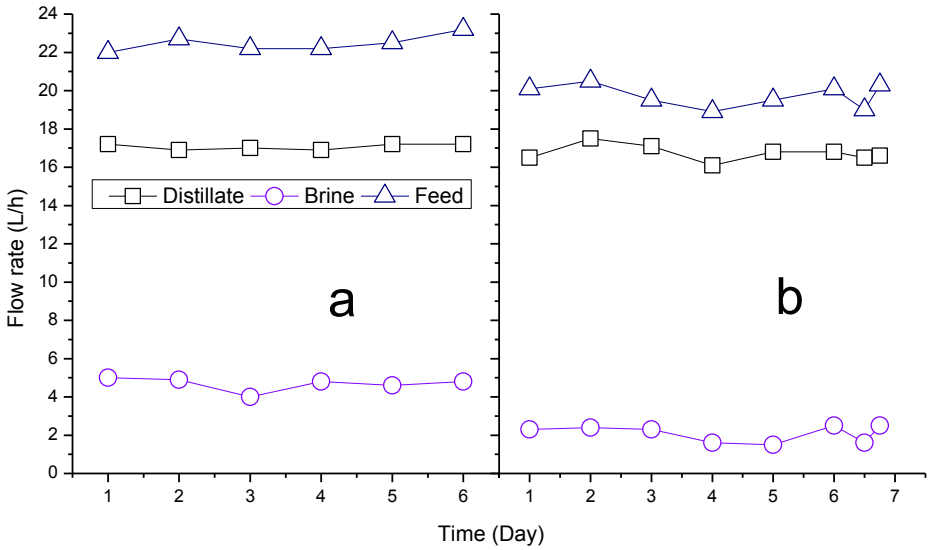

Figure 31: Distillate as a function of time: (a) WK03 and (b) CR06 (boiling point temperature = 75ºC and pressure chamber = 25 kPa absolute pressure).

4.3.2.2 Distillation production

4.3.2.2.1 Salt rejection

Salt rejection was a measure of conductivity (Figure 32). Figure 32 shows a gradual decline in conductivity for WK03 and CR06 distillates, and increased in the brine. The distillate conductivity for WK03 was lower than CR06, which were 0.022 and 0.030 mS/cm, respectively. The conductivity reading for the distillate was sometimes higher than the pervious. This is caused by carry-over of salt water droplets, which occurs from the high velocity vapour in the evaporation chamber [104]. Overall, the distillate is good and of high quality.

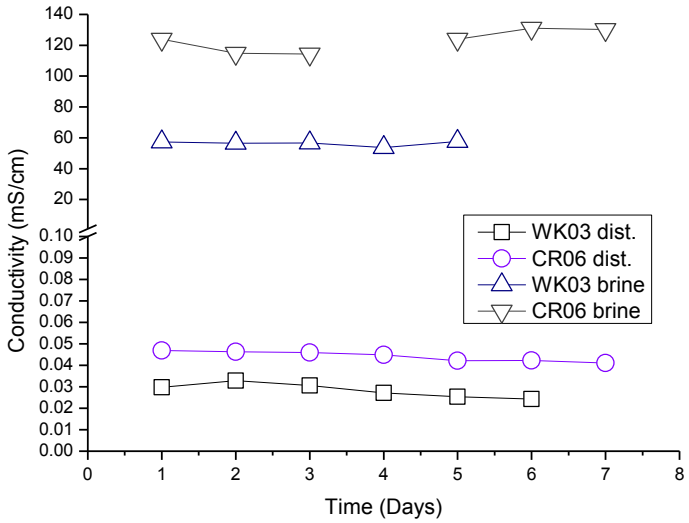

Figure 32: Conductivity as a function of time.

4.3.2.2.2 Distillate characteristics

The distillate characteristics for WK03 and CR06 are shown in Table 11 and Table 12. The distillate quality is also greater than the RO permeate. The rejection of ionic solids was 95% and above, with the exception of Mn^{2+}, which was 37.05%. However, Mn^{2+} was only 0.05 mg/L and is within satisfactory range [105]. In addition, the distillate conductivity and ionic contents met conditions for non-potable and potable reuse. Na^{2+} was the only physiochemical parameter to exceed 1 mg/L in both distillates, while K^{+} exceeded 1 mg/L in WK03.

Table 11: MED characteristics WK03 CSG water.

WK03 water (mg/L)								
	Na	Cl	Mg	Al	K	Ca	Mn	Fe
Feed brine	4449.84	186.48	12.87	13.76	38.99	40.31	0.13	144.3
MED conc.	21241.8	798.21	21.06	88.44	152.79	24.24	0.15	390.03
MED dist.	2.65	0.05	0.12	0.02	1.41	na	0.05	0.73
R (%)	99.8	99.92	97.49	99.73	95.15	na	37.05	98.32

Table 12: MED characteristics CR06 CSG water.

CR06 water (mg/L)								
	Na	Cl	Mg	Al	K	Ca	Fe	Si
Feed brine	6842	5604	17.67	0	33	13.67	3	68.33
MED conc.	68420	40867	3	2.5	293	6	6.5	410
MED dist.	1	0	0	0	0	0	0	0.5
R (%)	99.94	100	100	100	100	100	100	96.15

Note: Distillates are averaged from days one to five. Feed and MED brine is an average of day one and five.

Rejections of ionic solids (Table 11 and Table 12) are greater in CR06 than the former. However, the discrepancy is only 1.57%. Higher rejection could be attributed to the APS pre-treatment in CR06 experiment. Al^{2+} was 0 mg/L in CR06 feed brine, and increased 250 times in the MED. Throughout the pilot project, Al^{2+} was either very low or undetectable, which explains its negligence and appearance in the feed and MED brine, respectively.

Figure 33a and Figure 33b exhibits the pH for WK03 and CR06. The pH does not vary in distillates WK03 and CR06, and nor does it in the brines.

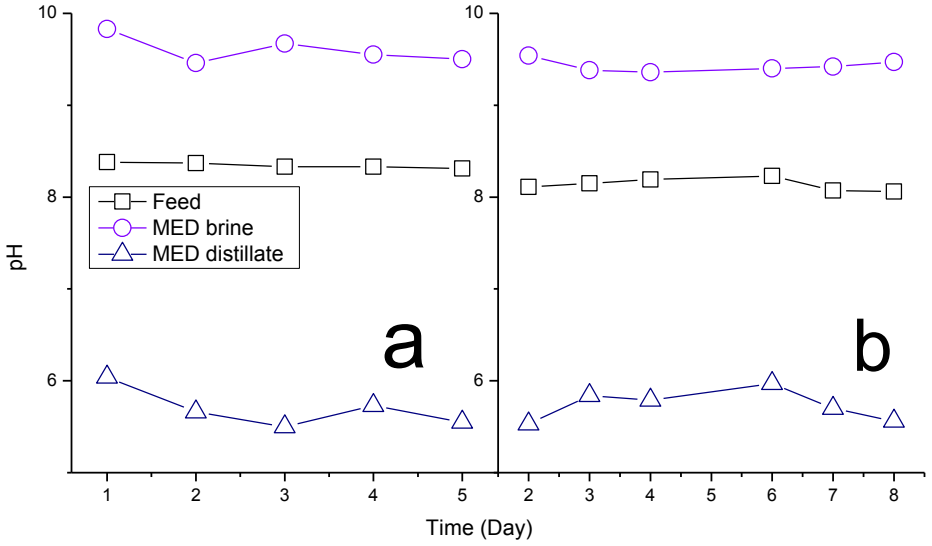

Figure 33: pH as a function of time: (a) WK03 and (b) CR06.

The pH is low and high for distillate and brine, respectively. This is identical to the RO process, because of fewer minerals to neutralise hydrogen ions, which is the effect of low distillate pH. The distillate pH is also lower than the RO permeate, because higher rejection of ionic solids.

4.3.2.3 Thermal-effect when increasing concentration ratio

Concentration ratio is a significant factor in MED processes, because it determines the recovery ratio of distillate from the source water – even to the point of "zero liquid discharge" [106]. The concentration ratio was set higher for CR06 compared to the former (see 4.3.2). The purpose of testing different and increasing concentration ratios was to boost the distillate production, and provide information on low discharge brine.

The results show increasing the concentration ratio was effective. For example, TDS in the feed brine was 13 mg/L and increases to 118 and 130 mg/L, when increasing its concentration from eight to 10 times, respectively (Figure 34). The MED brine is increased proportionally with the feed brine.

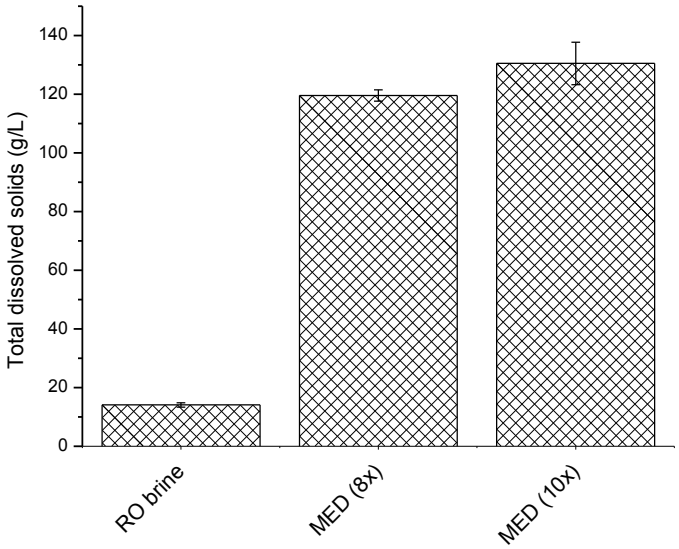

Figure 34: Total dissolved solids for CR06 RO and MED brine. MED (8x) represents water recovery 88.5% and MED (10x) represents water recovery set to 90%.

The brine produced from WK03 and CR06 were 611.7 L and 354.1 L. The brine from the latter is 42% less than the former, and confirms MED is possible at recovering further fresh water from CSG RO brines. In Table 11 and Table 12, the concentration of contaminants increased proportionally, except for Mg^{2+} and Ca^{2+} ions. Literature suggests that Mg^{2+} and Ca^{2+} to have precipitated and remained in the evaporation chamber, because concentration of the aforementioned ions are negligible in the distillate [107-109].

Though the MED had shown increasing concentration ratio is possible, treating high salt water with MED isn't unusual, because it is used for seawater treatment, which contains TDS five times more than brackish water sources (such as CSG water) [110]. Increasing concentration ratio has demonstrated fresh water recovery to increase a further 90% from CSG RO brine.

4.3.2.4 Thermal performance

4.3.2.4.1 Temperature

Figure 35 exhibits the temperature stability of the distillation process. Temperature stability for WK03 and CR06 show minor pockets of fluctuation. However, temperature distribution is observed stable throughout pilot experiments. The temperature of the feed is highest in CR06, precisely measuring at 71.8°C, whereas WK03, measured the lowest at 70.1°C. This equates a temperature difference of 1.7°C. The difference in feed temperature is accounted for the difference in feed water flow rate (see 4.3.2.1). Higher flow rate reduces the residence time of the feed. Low residence time also restricts the appropriate time for establishing thermal equilibrium in the distillation process [103, 109]. Flow rate was highest when treating WK03, which did not allow appropriate time for establishing a thermal equilibrium. The MED was effective in maintaining temperature for evaporating CSG RO brines.

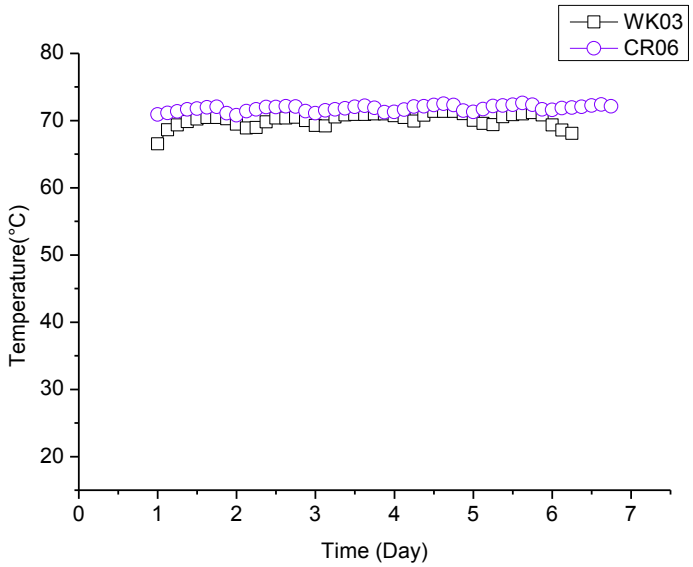

Figure 35: Operating feed temperature as a function of time: WK03 and CR06 CSG RO brine (pressure chamber = 25 kPa absolute pressure).

4.3.2.4.2 Heat transfer coefficient

Heat transfer coefficient is shown in Figure 36. Energy distribution is destabilised when the evaporator tubes are obstructed with scalants, which lowers the heat transfer area and distillate productivity. However, energy distribution was not interfered by deposits of scalants, because it remained stable throughout the evaporation process. However, heat transfer recorded its lowest on day six for CR06.

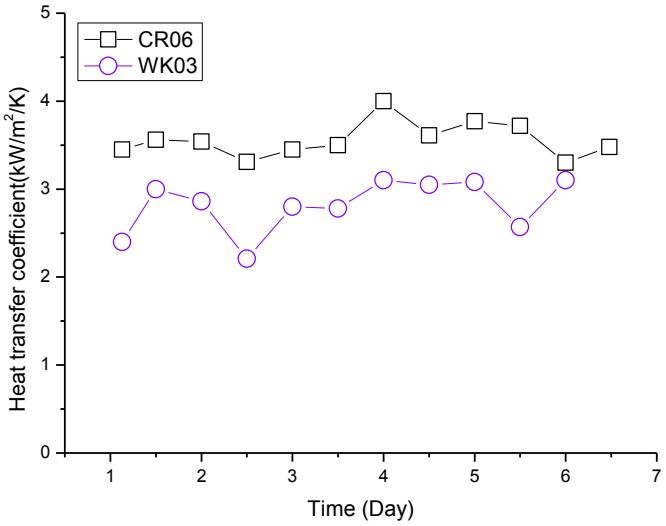

Figure 36: Heat transfer coefficient as a function of time (boiling point temperature = 75ºC and pressure chamber = 25 kPa absolute pressure).

The heat transfer, on most days, was 3 and 3.5 kW/m^2/K for WK03 and CR06. However, the heat transfer difference was 0.8 kW/m^2/K. The heat transfer coefficient can be altered with a changing temperature [107]. However, temperatures for WK03 and CR06 were not the cause for a heat transfer coefficient difference (see 4.3.2.4.1), because the temperature variance was 1.7°C. The concentration difference in WK03 and CR06 feed brine will increase the energy output. Because produced waters with higher TDS has lower availability of free water, which requires a greater demand of energy for the evaporation process. This was evident on day four, when CR06 heat transfer increased to 4 kW/m^2/K, because concentration ratio increased from eight to 10 times, which also increases distillate productivity, thus increasing heat supply [106]. However, the heat transfer remained consistent at high water recovery from CSG RO brine.

4.3.2.5 Scaling mitigation by pre-treatment protocol

Scaling by divalent ions is manageable with a conventional pre-treatment protocol. However, when achieving higher water recovery, an appropriate APS pre-treatment

is required, because chances are higher for precipitation of scalants. An APS pre-treatment was executed for CR06 RO brine treatment, because the water recovery was higher than the former. Overall, scaling did not limit the MED performance; because both experiments were steady (see sections 4.3.2.2, 4.3.2.4.1 and 4.3.2.4.2). This section explains prevention of scaling with respects to the pre-treatment protocol.

Figure 37 and Figure 38 presents scale formation for WK03 and CR06, and is drawn by the fact that the evaporation glass is clearer in earlier operating days than the latter.

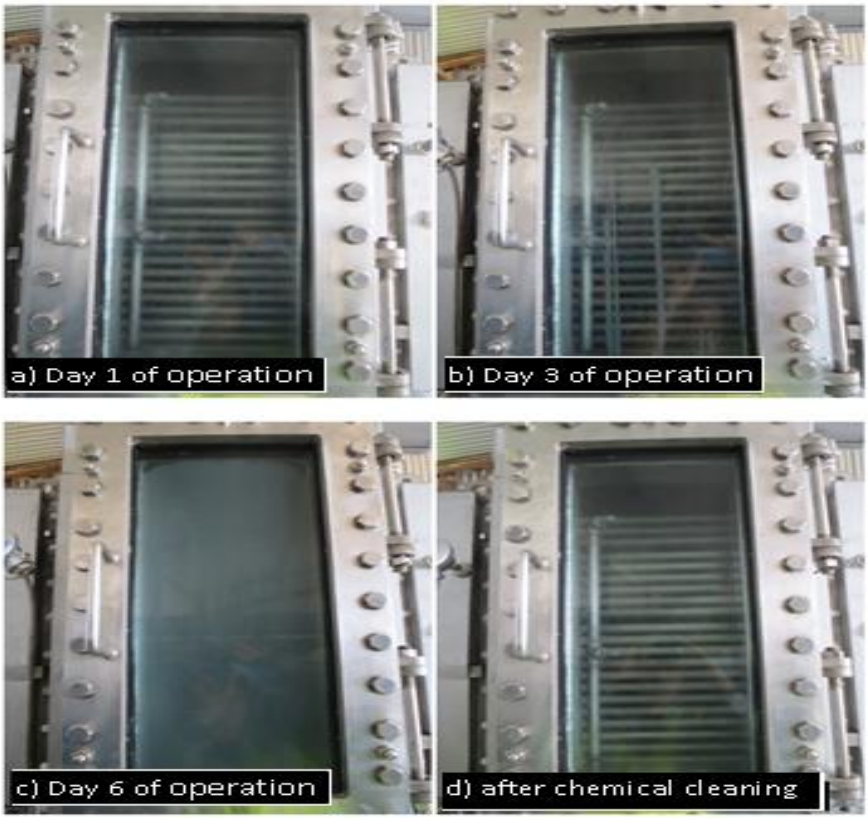

Figure 37: MED evaporator glass casing when treating WK03 CSG RO brine.

Figure 38: MED evaporator glass casing when treating CK06 CSG RO brine.

WK03 (Figure 37), shows minimal precipitation of scalant on the glass casing in earlier operating days. This pattern is the same for CR06 (Figure 38). White clouds (scalants) were denser for WK03 with minimal chipping on the top end corners of the glass casing, while they were lighter for CR06 with intense chipping. The intense chipping observed (Figure 38) was accounted for increasing concentration ratio made on operating day four. Scalants were removed easily, even after the lengthy operation. The pre-treatment protocols were effective to maintain a stable MED (see 4.3.2.1); even though scalant deposits on the glass case were severe.

4.4 Feasibility consideration

Unlike RO, MED requires two forms of energy: (1) heat, which demonstrates largest portion of energy input (Table 13) and (2) electricity – required for pumps and other electrical components [111]. Energy consumption is not calculated in this study, because no energy-recovery unit was equipped with the MED unit. However, energy demand has shown to be intensive in past studies, especially when MED is not

coupled with renewable energy. The energy consumption for low salt desalination is provided in Table 13.

Table 13: Energy consumption of RO and MED for brackish desalination.

Application	Energy demand	Consumption (kW h/ m^3)	Ref.
RO	Electricity	0.5 – 2.0	[112]
		1.5 – 2.5	[111]
		1.0 – 2.5	[113]
MED	Electricity	1.1 – 4.5	[112]
		2.0 – 2.5	[111]
		2.5 – 2.9	[113]
	Heat	25 – 165	[112]
		40 – 64	[111]
		4.5 – 6.5	[113]

The application of MED should be considered on the scale of water production, because this determines costs associated in production and capital. Literature illustrates the capacity of plant from 91,000 m^3 to 320,000 m^3 and 100m^3 and less have associated costs from 0.52 to 1.01 [114, 115], and 2.4 to 9.6 \$/m^3 [116], respectively. Larger plants are more cost effective, because renewable energy technology are built and designed more efficient, than those renewable technology for smaller scale plants [117]. These figures were extracted from 1999 – 2006, and are outdated. However, the trend in higher associated costs in smaller compared to larger plants is still credible, with most recent and older installation being less and most expensive, respectively, due to earlier technology being less advanced than the latter [118].

An alternative option to MED is a seawater RO system. Seawater RO systems are capable to further recover water and lower operational costs, associated in MED desalination. Seawater RO membranes are durable and can withstand harsher conditions, thus, effectively increasing water recovery and lowering the consumption of energy and costs, associated with MED. In addition, the RO permeate and MED

distillate are of high quality, which could be blended with UF filtrate to reduce the volume of treated water, and subsequently lower the associated production costs (Figure 39a and Figure 39b).

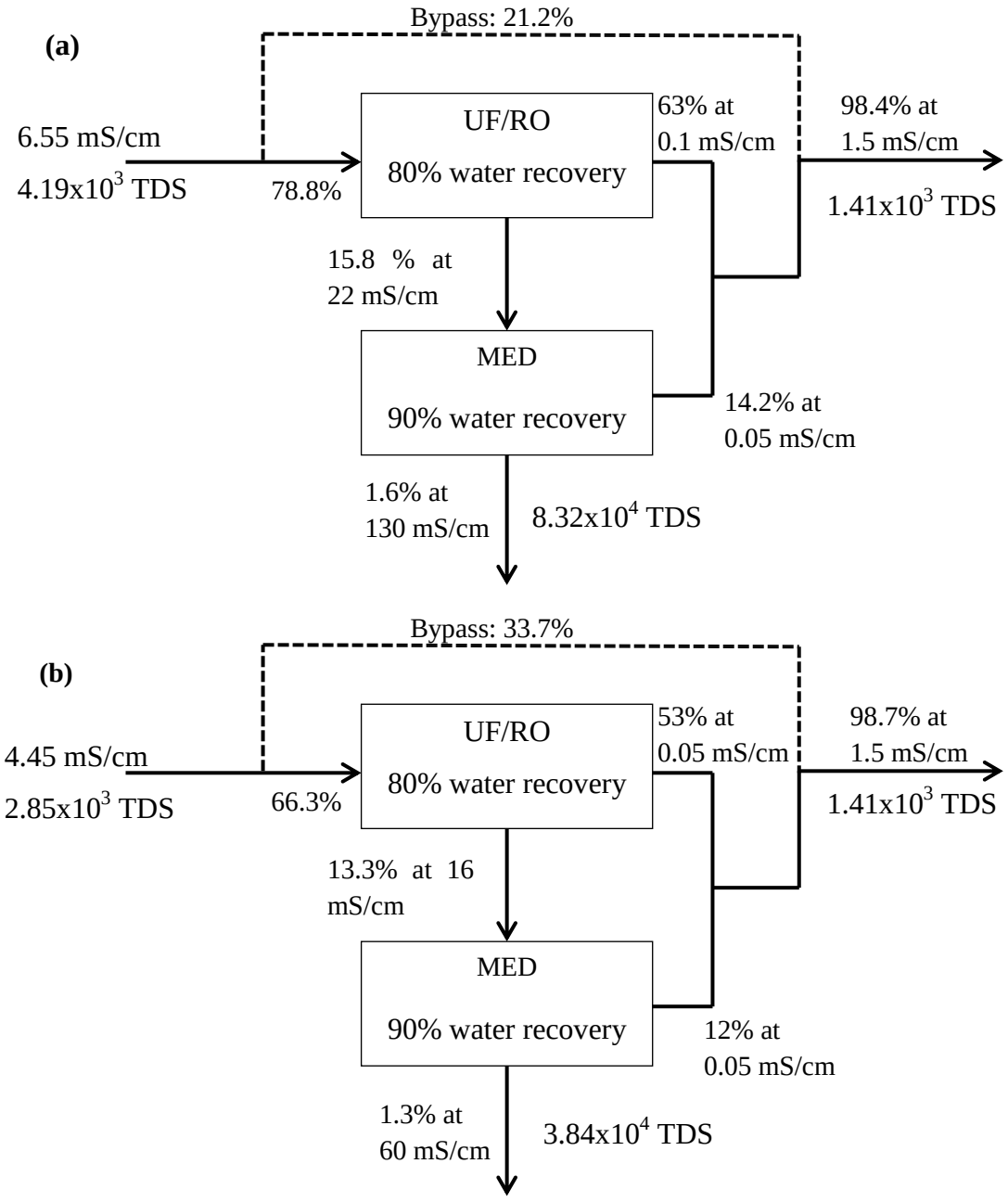

Figure 39: a) Possible water balance for a combined RO MED treatment plant using water from the (a) CR06 well and (b) the WK03 well if the produced water is to be used for irrigation. The water recovery rates of the RO system is optimised in terms of energy consumption. TDS are in units of mg/L.

Whether seawater RO or a MED system is implemented, associated brine is inevitable, and the volume is contingent on the set recovery. However, producing NaOH from CSG MED brine has been proven feasible using membrane electrolysis. This will off-set cost associated in the CSG brine management and a profitable product. In fact, this is a responsible management solution for managing CSG water, recommended by Authorities, to minimise the volume of water for disposal [7].

4.5 Suitability for discharge

Permeate and distillate suitability will be examined against Primary Industries National Standards [105, 119]. The SAR for permeate and distillate recovery is presented in Table 14.

Gloucester, NSW, has an agriculture industry in beef-cattle and dairy. The produced water treated by the MED system could be used for beneficial use, such as irrigation and livestock in the town farms. It is noteworthy that agricultural practices in Australia are based where limited rainfall is available, and groundwater is the main source of irrigation. CSG operators in Gloucester should cooperate with local farmers, to provide re-useable water.

Table 14: SAR calculation from the clean water product.

	SAR (meq/L)	Conductivity (mS/cm)
RO permeate		
WK03	1.92	0.04
CR06	1.92	0.08
MED distillate		
WK03	0.75	0.03
CR06	∞	0.04

4.5.1 Irrigation

CSG-produced waters from Gloucester exceed primarily in Na^{2+}, requiring pre-treatment before committed to useful practises. For instance, the SAR for WK03 and CR06 permeate was 1.92 meq/L, and the distillate was 0.75 and infinite (∞) mg/L, respectively. The SAR for CR06 distillate is higher, because, Ca^{2+} and Mg^{2+} ions were negligible, and minor in concentration for WK03.

SAR and its relationship to salinity (conductivity) (see 4.1), will assess the permeate and distillate discharge suitability. Electrolytes (conductivity) for WK03 and CR06 permeates was 0.04 and 0.08 mS/cm, and 0.03 and 0.04 mS/cm for the distillate (Table 14). Severe soil degradation will result if the permeate and distillate is used directly, because Na^{2+} ions proportional to conductivity is too high [3]. The clean water produced by RO and MED is too pure, for discharge. Minerals (i.e.Mg^{2+} and Ca^{2+}) affixed to permeate and distillates will elevate the conductivity and lower the soil deformation potential.

Cl^- ions can be concerning to ecology. For example, Cl^- exceeding 40 mg/L will degrade leaves, due to low metabolic processes. When concentration of Cl^- is between 350 to 750 mg/L, plants will uptake Cd^{2+}, which reduces intake of essential nutrients (i.e. K^+) and crop yield [120]. However, Cl^- in the RO permeate and MED distillate is less than 1 mg/L, having no effect to ecology.

Al^{3+}, Mn^{2+} and Fe^{2+}/Fe^{3+} should not exceed 20, 10 and 10 mg/L, respectively, for short term effects to soil structures [105]. In the RO permeate and MED distillate, the aforementioned ions does not present a threat for irrigation practice, because they are below the Australian standards.

The pH for irrigation waters should be between 6.5 to 8.4. Water pH outside this range would proceed in nutritional imbalances and toxic ions. The pH for WK03 and CR06 MED distillate were 6.04 to 5.50 and 5.97 to 5.53, which makes this unsuitable. The RO permeate pH for WK03 was also below 6.5, except on day two (see 4.3.1.2.2). The pH for CR06 permeate was again higher on other days. The pH on days one through to five and eight showed the water pH to be acceptable while

days six, seven and nine did not. Introducing minerals to both permeate and distillate would elevate pH balance for irrigation.

4.5.2 Livestock

Livestock are more tolerable to dissolved ionic solids compared to plant roots and soil systems. Inorganics such as Ca^{2+} and Mg^{2+} are essential ions for stock nutrition and diet, if they should not exceed 1,000 and 2,000 mg/L, respectively. In the RO permeate and MED distillate, Ca^{2+} and Mg^{2+} did not exceed 0.90 mg/L. Mg^{2+} and Ca^{2+} in the untreated WK03 and CR06 CSG water also met livestock requirements (see 4.1).

Table 15 shows the decreasing order of TDS tolerance to livestock [105]. The TDS in untreated CSG water were suitable for all except for poultry and dairy cattle (see also 4.1 for TDS comparison to Table 15). The TDS in RO permeate and MED distillate was calculated using the following equation:

Table 15: TDS in water for livestock tolerance [105].

TDS (mg/L)			
Livestock	No effects	Possible effects*	Observable effects[#]
Beef cattle	0 – 4,000	4,000 – 5,000	5,000 – 10,000
Dairy cattle	0 – 2,500	2,500 – 4,000	4,000 – 7,000
Sheep	0 – 5,000	5000 – 10,000	10,000 – 13,000[b]
Horses	0 – 4,000	4,000 – 6000	6,000 – 7,000
Pigs	0 – 4,000	4,000 – 6,000	6,000 – 8,000
Poultry	0 – 2,000	2,000 – 3,000	3,000 – 4,000

*Animals will not drink water at the start but will gradually adapt.

[#]Loss of production and lowered animal health.

$$TDS_{(mg/L)} = EC\ (^{mS}/_{cm}) \times 670 \qquad \text{Eq. 5}$$

TDS for WK03 and CR06 RO permeate and MED distillate was 33.5 and 67, and 13.4 and 26.8 mg/L, respectively. The TDS levels lies in the category where no effects to animals would occur. However: reintroducing water of poorer quality to stock diet becomes difficult, when high quality water has been consumed for long periods [105].

Mn^{2+} and Fe^{2+}/Fe^{3+} in WK03 and CR06 CSG-produced waters do not pose a threat to livestock health, as they are not sufficiently toxic, while Al^{3+} should not exceed 5 mg/L [105]. Al^{3+} in the RO permeate and MED distillate were 0 to 0.03 mg/L, and 7.53 and 0.01 mg/L in untreated WK03 and CR06, respectively. Al^{3+} in untreated WK03 exceeds Australian standards by 2.53 mg/L, and would require conditioning before introducing into livestock diet.

CHAPTER 5: CONCLUSIONS AND RECOMMENDATIONS

5.1 Conclusion

This study evaluated the MED process to further minimise the volume of CSG RO brine at a pilot scale level. The conclusion of this study was drawn as below.

CSG-produced waters were obtained from two exploration sites in the Gloucester basin, namely Waukivory 03 (WK03) and Craven 06 (CR06). The WK03 and CR06 gas-wells have the lowest and highest salinity levels from the Gloucester gas field, respectively. The brine produced from the RO was then treated with MED, and its process stability showed confidence in steady distillate productivity. The MED was also capable at increasing water recovery from eight to 10 times of the concentration ratio. Up to 91% of fresh water can be extracted from RO brine by MED, which was contingent on the APS pre-treatment protocol. The MED process achieved a near complete salt rejection (i.e. >99.99%), which was measured by electrical conductivity. The thermal output was stable, even when the concentration ratio had increased. However, the thermal output did show evidences of minor decline, when the water recovery set to increase had operated after a 24 hour period. Scaling might have occurred as evident by the slow decline of distillate productivity and heat transfer area. The composition of the MED brine increased proportionally with water recovery, except for Ca^{2+}, which had precipitated possibly in the MED brine.

Both RO permeate and MED distillate was of high quality. The permeate and distillate is suitable for blending with untreated CSG produced water for irrigation, livestock watering and a range of other beneficial uses.

5.2 Recommendations

Several recommendations (see 4.5) were proposed for a more efficient and practical MED setup. If a MED is installed, it is recommended a blending ratio (where distillate and permeate are blended with untreated CSG water) is implemented, because this approach reduces the management of brine, thus reducing energy consumption. However, if further water recovery is still desired, and RO is the only option, it is recommended seawater RO membranes be used to treat CSG RO brine. This approach would reduce additional capital and operational costs associated with the MED process. Furthermore: seawater RO membranes compared to standard brackish RO membranes can withstand harsher conditions and capable to recovering more water.

The main limitation in this study was a detailed economic analysis. The MED system lacked an energy-recovery unit, which could have provided statistical evidence on raw output data. Thus, for further studies, it is recommended that energy consumption be suitably investigated. This would serve to inform the future design of energy-efficient CSG water treatment plants.

CSG water contains various salts such as, Na^+, K^+ and HCO_3^-. Na^+, in particular, is concerning, which will cause infiltration problems and deteriorate soils if discharged directly into soil systems. Research into mineral extraction is highly recommended for investigation into zero liquid discharge and reducing soil profile breakdowns. This approach is plausible, as [43] have shown it possible to extract caustic soda from CSG brine. Penrice Soda is pending their research into soda ash extraction. It would be encouraging to investigate soda ash reclamation for future research, as this possibility is still uncertain.

CHAPTER 6: REFERENCES

1. Abousnina, R.M., *Oily wastewater treatment: removal of dissolved organic components by forward osmosis*, in *School of Civil, Mining and Environmental Engineering*. 2012, University of Wollongong: University of Wollongong.
2. Beletse, Y.G., et al., *Can crops be irrigated with sodium bicarbonate rich CBM deep aquifer water? Theoretical and field evaluation.* Ecological Engineering, 2008. **33**(1): p. 26-36.
3. Nghiem, L.D., et al., *Treatment of coal seam gas produced water for beneficial use in australia: A review of best practices.* Desalination and Water Treatment, 2011. **32**(1-3): p. 316-323.
4. Origin. *Coal seam gas production and the Great Artesian basin*. 2013, Australian Pacific LNG. ConocoPhilips. [cited 2014 12 November]; Available from: www.aplng.com.au/.
5. Ahmed, M., et al., *Use of evaporation ponds for brine disposal in desalination plants.* Desalination, 2000. **130**(2): p. 155-168.
6. Ahmed, M., et al., *Brine disposal from reverse osmosis desalination plants in Oman and the United Arab Emirates.* Desalination, 2001. **133**(2): p. 135-147.
7. Department of Environment and Heritage Protection, *Coal Seam Gas Water Management Policy*. 2012, Queensland Government: Brisbane.
8. Li, C., Y. Goswami, and E. Stefanakos, *Solar assisted sea water desalination: A review.* Renewable and Sustainable Energy Reviews, 2013. **19**(0): p. 136-163.
9. Cook, P., et al., *Engineering Energy: Unconventional Gas Production*, in *Report for the Australian Council of Learned Academies*. 2013: Melbourne.
10. IEA, *World Energy Outlook*, in *International Energy Agency*. 2012: Paris, France.
11. Department of Natural Resources and Mines, *Coal seam gas overview*. 2014, Queensland Government: Brisbane.
12. *BP Statistical revew of World Energy*. St James's Square, London. p. 48.

13. Geoscience Australia, *Coal Seam Gas*, M.C. Australia, Editor. 2012, Australian Government: Canberra.
14. Faiz, M., et al., *The influence of petrological properties and burial history on coal seam methane reservoir characterisation, Sydney Basin, Australia.* International Journal of Coal Geology, 2007. **70**(1): p. 193-208.
15. Hamawand, I., T. Yusaf, and S.G. Hamawand, *Coal seam gas and associated water: A review paper.* Renewable and Sustainable Energy Reviews, 2013. **22**: p. 550-560.
16. Department of Industry, *Energy in Australia*. 2011, Australian Government: Canberra.
17. Shen, J., et al., *Relative permeabilities of gas and water for different rank coals.* International Journal of Coal Geology, 2011. **86**(2): p. 266-275.
18. Moore, T.A., *Coalbed methane: A review.* International Journal of Coal Geology, 2012. **101**: p. 36-81.
19. Van Voast, W.A., *Geochemical signature of formation waters associated with coalbed methane.* AAPG bulletin, 2003. **87**(4): p. 667-676.
20. U.S. Geological Survey. *Water Produced with Coal-Bed Methane*. Science for a changing world [Online] 2000 accessed 23/04/2014]; Available from: http://pubs.usgs.gov/fs/fs-0156-00/fs-0156-00.pdf.
21. Taulis, M. and M. Milke, *Coal Seam Gas Water from Maramarua, New Zealand: Characterisation and Comparison to United States Analogues.* Journal of Hydrology (New Zealand), 2007. **46**(1): p. 1-17.
22. Jackson, R.E. and K.J. Reddy, *Trace Element Chemistry of Coal Bed Natural Gas Produced Water in the Powder River Basin, Wyoming.* Environmental Science & Technology, 2007. **41**(17): p. 5953-5959.
23. Jackson, R.E. and K.J. Reddy, *Geochemistry of Coalbed Natural Gas (CBNG) Produced Water in Powder River Basin, Wyoming: Salinity and Sodicity.* Water, Air, and Soil Pollution, 2007. **184**(1): p. 49-61.
24. Wright, J.M., A. Colling, and G. Bearman, *Seawater: Its Composition, Properties and Behaviour: Prepared by an Open University Course Team*. 2013: Elsevier Science.

25. Dahm, K.G., et al., *Composite geochemical database for coalbed methane produced water quality in the Rocky Mountain region.* Environmental science & technology, 2011. **45**(18): p. 7655-7663.
26. Brinckerhoff, P., *Flow Testing of Craven 06 and Waukivory 03 Gas Wells*, in *2162406C-WAT-RPT-7642 RevB*. 2013, Parsons Brinkerhoff: Sydney.
27. Wang, X., et al., *The effect of zeolite treatment by acids on sodium adsorption ratio of coal seam gas water*. Water research, 2012. **46**(16): p. 5247-5254.
28. Johnston, C.R., *Soil Chemical and Physical Changes Resulting from Irrigation with Coalbed Natural Gas Co-produced Water: Effects of Soil Amendments and Water Treatments*. 2007, University of Wyoming. Department of Renewable Resources: ProQuest. 76 pages.
29. Menneer, J.C., C.D.A. McLay, and R. Lee, *Effects of sodium-contaminated wastewater on soil permeability of two New Zealand soils.* Soil Research, 2001. **39**(4): p. 877-891.
30. Dikinya, O., C. Hinz, and G. Aylmore, *Influence of sodium adsorption ratio on sodium and calcium breakthrough curves and hydraulic conductivity in soil columns.* Australian Journal of Soil Research, 2007. **45**(8): p. 586-597.
31. CSRIO. *Coal seam gas*. Produced water and site management [Online] 2012 accessed 23/04/2014]; Available from: www.csiro.au.
32. NETL, *Powder River Basin coalbed methane development and produced water management study*. 2002, U.S. Department of Energy: Office of Fossil Energy and National Energy Technology Laboratory Strategic Center for Natural Gas.
33. Khan, S. and G. Kordek, *Coal Seam Gas: Produced Water and Solids*, in *Prepared for the Office of the NSW Chief Scientist and Engineer (OCSE)*. 2013, School of Civil Environmental Engineering, UNSW: Sydney. p. 6 - 59.
34. Womersley, J., *Approval of coal seam gas water for beneficial use*. 2011, Queensland Department of Environmental and Recourse Management: Brisbane. p. 1 - 37.
35. Zheljazkov, V.D., et al., *The effect of coal-bed methane water on spearmint and peppermint.* Journal of Environmental Quality, 2013. **42**(6): p. 1815-1821.

36. Aravinthan, V. and D. Harrington, *Coal seam gas water as a medium to grow Dunalliella tertiolecta microalgae for lipid extraction.* Desalination and Water Treatment, 2013: p. 1-12.
37. Pratt, S., et al. *The potential for generating algae derived biofuels using coal seam gas water as the growth media*. in *IWA conference on water and industry*. November 2009. Palmerston North, New Zealand: University of Queensland.
38. Buchanan, J.J., et al., *Algal growth and community structure in a mixed-culture system using coal seam gas water as the water source.* Environmental technology, 2013. **34**(6): p. 695-701.
39. Angino, E.E., *Selective Element Recovery from Oil Field Brines.* Water Resources Research, 1970. **6**(5): p. 1501-1504.
40. Tallmadge, J.A., J.B. Butt, and H.J. Solomon, *Minerals From SeaA Salt.* Industrial & Engineering Chemistry, 1964. **56**(7): p. 44-65.
41. Melián-Martel, N., J.J. Sadhwani, and S. Ovidio Pérez Báez, *Saline waste disposal reuse for desalination plants for the chlor-alkali industry.* Desalination, 2011. **281**: p. 35.
42. Melián-Martel, N., J.J. Sadhwani Alonso, and S.O. Pérez Báez, *Reuse and management of brine in sustainable SWRO desalination plants.* Desalination and Water Treatment, 2012. **51**(1-3): p. 560-566.
43. Simon, A., et al., *Sodium hydroxide production from sodium carbonate and bicarbonate solutions using membrane electrolysis: A feasibility study.* Separation and Purification Technology, 2014. **127**(0): p. 70-76.
44. Grimaldi, M.C., et al., *Produced Water Reuse for Production of Chemicals*, in *SPE International Conference on Health, Safety and Environment in Oil and Gas Exploration and Production*. 12-14 April 2010, Society of Petroleum Engineers: Rio de Janeiro, Brazil. p. 2637-2641.
45. Penrice Soda, *GE and Penrice Consortium to trial converting coal seam gas brine into saleable products*, in *Consortium to Build Brine Pilot Plant (BPP) to Selectively Precipitate and Recover Salts from CSG Brine Streams*. 2011, Penrice Soda Holdings Limited: Adelaide, Australia.
46. Morrin, M., *An appetite for soda ash.* Glass (Redhill), 2006. **83**(11): p. 30.

47. Morrin, M., *Oversupply characterises current soda ash industry*. Glass international, 2010. **33**(9): p. 25-26.
48. Gahlaut, S., *Chinese container glass leads the way with rapid growth.* Glass international, 2011. **34**(3): p. 21-26.
49. Gahlaut, S., *Raw materials and their place in the global market.* Glass international, 2010. **33**(9): p. 21-24.
50. Kostick, D.S., *2011 Minerals Yearbook*, in *Soda Ash [ADVANCE RELEASE]*. 2012, USGS: U.S. p. 11.
51. Penrice Soda, *"Pro Asia Pacific" soda ash joint venture commences*, in *ASX/ Press Release*. 2013, Penrice Soda Holdings Limited: Adelaide, Australia.
52. Orica. *Orica Chemicals Australia*. 2014 Online accessed 18/05/2014]; Available from: http://www.chemicalsaustralia.com.au/.
53. IHS Chemicals, *Chlorine/Sodium Hydroxide*. 2011: U.S.
54. Geoscience Australia, *Aluminium*, e.a.t. Department of recourses, Editor. 2012, Australian Government: Canberra.
55. Ratnayaka, D.D., M.J. Brandt, and M. Johnson, *Water Supply*. 6th ed. 2009: Butterworth-Heinemann. 744 pages.
56. Abdulgader, H.A., V. Kochkodan, and N. Hilal, *Hybrid ion exchange - Pressure driven membrane processes in water treatment: A review.* Separation and Purification Technology, 2013. **116**: p. 253-264.
57. Welch, J., *Reverse osmosis treatment of CBM produced water continues to evolve.* Oil Gas J, 2009. **107**(37): p. 45-50.
58. Lee, K.P., T.C. Arnot, and D. Mattia, *A review of reverse osmosis membrane materials for desalination—Development to date and future potential.* Journal of Membrane Science, 2011. **370**(1): p. 1-22.
59. Johnson, J. and M. Busch, *Engineering Aspects of Reverse Osmosis Module Design.* Desalination and Water Treatment, 2010: p. 236-248.
60. Al-Obaidani, S., et al., *Potential of membrane distillation in seawater desalination: Thermal efficiency, sensitivity study and cost estimation.* Journal of Membrane Science, 2008. **323**(1): p. 85-98.
61. Qtaishat, M.R. and F. Banat, *Desalination by solar powered membrane distillation systems.* DESALINATION, 2013. **308**: p. 186-197.

62. Averina, A., M.G. Rasul, and S. Begum, *Management of Coal Seam Gas (CSG) By-Product Water: A Case Study on Spring Gully Mine Site in Queensland, Australia*, in *2nd International Conference on Waste Management, Water Pollution, Air Pollution, Indoor Climate (WWAI'08)*. 2008, Central Queensland University: Corfu, Greece. p. 169 - 174.
63. Al-Shammiri, M. and M. Safar, *Multi-effect distillation plants: state of the art.* Desalination, 1999. **126**(1–3): p. 45-59.
64. Michels, T., *Recent achievements of low temperature multiple effect desalination in the western areas of Abu Dhabi. UAE.* Desalination, 1993. **93**(1–3): p. 111-118.
65. Joo, H.-J. and H.-Y. Kwak, *Performance evaluation of multi-effect distiller for optimized solar thermal desalination.* Applied Thermal Engineering, 2013. **61**(2): p. 491-499.
66. Awerbuch, L.A. *Vision for Desalination–Challenges and Opportunities*. in *Proceedings of the IDA World Congress and Water Reuse*. March 8–13, 2002. Manama, Bahrain.
67. Ophir, A., A. Gendel, and R.R. Kalantary, *The LT -MED process for SW Cogen Plants.* Desalination Water Reuse, 1994. **4**(1): p. 28 - 31.
68. McCabe, W.L., J. Smith, and P. Harriott, *Unit Operations of Chemical Engineering*. 2001: McGraw-Hill Education.
69. Ophir, A. and A. Gendel, *Steam driven large multi effect MVC (SD MVC) desalination process for lower energy consumption and desalination costs.* Desalination, 2007. **205**(1–3): p. 224-230.
70. Alkhudhiri, A., N. Darwish, and N. Hilal, *Membrane distillation: A comprehensive review.* Desalination, 2012. **287**: p. 2-18.
71. Susanto, H., *Towards practical implementations of membrane distillation.* Chemical Engineering & Processing: Process Intensification, 2011. **50**(2): p. 139-150.
72. Guillén-Burrieza, E., et al., *Experimental analysis of an air gap membrane distillation solar desalination pilot system.* Journal of Membrane Science, 2011. **379**(1): p. 386-396.
73. Xu, Y., B.-k. Zhu, and Y.-y. Xu, *Pilot test of vacuum membrane distillation for seawater desalination on a ship.* Desalination, 2006. **189**(1): p. 165-169.

74. Martínez, L. and J.M. Rodríguez-Maroto, *Membrane thickness reduction effects on direct contact membrane distillation performance.* Journal of Membrane Science, 2008. **312**(1): p. 143-156.
75. Laganà, F., G. Barbieri, and E. Drioli, *Direct contact membrane distillation: modelling and concentration experiments.* Journal of Membrane Science, 2000. **166**(1): p. 1-11.
76. Schofield, R.W., A.G. Fane, and C.J.D. Fell, *Heat and mass transfer in membrane distillation.* Journal of Membrane Science, 1987. **33**(3): p. 299-313.
77. Martinetti, C.R., A.E. Childress, and T.Y. Cath, *High recovery of concentrated RO brines using forward osmosis and membrane distillation.* Journal of Membrane Science, 2009. **331**(1): p. 31-39.
78. Osman, M.S., J.J. Schoeman, and L.M. Baratta, *Desalination/concentration of reverse osmosis and electrodialysis brines with membrane distillation.* Desalination and Water Treatment, 2010. **24**(1-3): p. 293-301.
79. Mericq, J.-P., S. Laborie, and C. Cabassud, *Vacuum membrane distillation of seawater reverse osmosis brines.* Water Research, 2010. **44**(18): p. 5260-5273.
80. Teoh, M.M. and T.-S. Chung, *Membrane distillation with hydrophobic macrovoid-free PVDF–PTFE hollow fiber membranes.* Separation and Purification Technology, 2009. **66**(2): p. 229-236.
81. Feng, C., et al., *Preparation and properties of microporous membrane from poly(vinylidene fluoride-co-tetrafluoroethylene) (F2.4) for membrane distillation.* Journal of Membrane Science, 2004. **237**(1): p. 15-24.
82. Song, L., et al., *Pilot plant studies of novel membranes and devices for direct contact membrane distillation-based desalination.* Journal of Membrane Science, 2008. **323**(2): p. 257-270.
83. El-Nashar, A.M., *Multiple Effect Distillation of Seawater Using Solar Energy*. Illustrative ed. 2009, University of California: Nova Science Pub Incorporated. 112 pages.
84. Saidur, R., et al., *An overview of different distillation methods for small scale applications.* Renewable and Sustainable Energy Reviews, 2011. **15**(9): p. 4756-4764.

85. Ophir, A. and F. Lokiec, *Advanced MED process for most economical sea water desalination.* Desalination, 2005. **182**(1): p. 187-198.
86. IDE Technologies. *Your Partners in Thermal Desalination*. Multi-Effect Distillation (MED) [Online] 2013 accessed 03/06/2014]; Available from: http://www.ide-tech.com.
87. Bouška, V., *Geochemistry of coal*. 1981: Elsevier Scientific Pub. Co. 284.
88. Rice, C.A., et al., *Chemical and stable isotopic evidence for water/rock interaction and biogenic origin of coalbed methane, Fort Union Formation, Powder River Basin, Wyoming and Montana U.S.A.* International Journal of Coal Geology, 2008. **76**(1): p. 76-85.
89. Benko, K.L. and J.E. Drewes, *Produced Water in the Western United States: Geographical Distribution, Occurrence, and Composition.* Environmental Engineering Science, 2008. **25**(2): p. 239-246.
90. Pashin, J.C., *Hydrodynamics of coalbed methane reservoirs in the Black Warrior Basin: Key to understanding reservoir performance and environmental issues.* Applied Geochemistry, 2007. **22**(10): p. 2257-2272.
91. Cheung, K., et al., *Produced fluids and shallow groundwater in coalbed methane (CBM) producing regions of Alberta, Canada: Trace element and rare earth element geochemistry.* International Journal of Coal Geology, 2009. **77**(3): p. 338-349.
92. Arrow Energy, *Underground Water Impact Report - For Authority to Prospect 1103*. 2013: Queensland.
93. Worley Parsons, *Spatial Analysis of Coal Seam Gas Water Chemistry*. 2012.
94. Alawadhi, A.A., *Pretreatment plant design — Key to a successful reverse osmosis desalination plant.* Desalination, 1997. **110**(1): p. 1-10.
95. Rachman, R.M., et al., *Assessment of silt density index (SDI) as fouling propensity parameter in reverse osmosis (RO) desalination systems.* Desalination and Water Treatment, 2012. **51**(4-6): p. 1091-1103.
96. Yongping, H. and L. Qiang. *Effects of Colloidal Fouling and Concentration Polarization on RO Membrane Performance*.
97. Grossman, G. and A.A. Sonin, *Experimental study of the effects of hydrodynamics and membrane fouling in electrodialysis.* Desalination, 1972. **10**(2): p. 157-180.

98. Rajan, K.S., et al., *Electrodialytic demineralization of brackish waters by using inorganic ion-exchange membranes.* Desalination, 1968. **5**(3): p. 371-390.
99. Sheikholeslami, R. and S. Zhou, *Performance of RO membranes in silica bearing waters.* Desalination, 2000. **132**(1-3): p. 337-344.
100. Sahachaiyunta, P., T. Koo, and R. Sheikholeslami, *Effect of several inorganic species on silica fouling in RO membranes.* Desalination, 2002. **144**(1-3): p. 373-378.
101. Sheikholeslami, R. and S. Tan, *Effects of water quality on silica fouling of desalination plants.* Desalination, 1999. **126**(1-3): p. 267-280.
102. Gabelich, C.J., et al., *The role of dissolved aluminum in silica chemistry for membrane processes.* Desalination, 2005. **180**(1-3): p. 307-319.
103. Dey, P.K., et al., *Performance of a single-effect desalination system operating with different tube profiles and materials.* Desalination, 2004. **166**(0): p. 69-78.
104. Kafi, F., et al., *New MED plate desalination process: thermal performances.* Desalination, 2004. **166**: p. 53-62.
105. Australian and New Zealand guidelines for fresh and marine water quality. Volume 1, *The guidelines / Australian and New Zealand Environment and Conversation Council, Agriculture and Resource Management Council of Australia and New Zealand.* 2000.
106. Zhao, D., et al., *Theoretical analyses of thermal and economical aspects of multi-effect distillation desalination dealing with high-salinity wastewater.* Desalination, 2011. **273**(2–3): p. 292-298.
107. Aly, N.H. and A.K. El-Figi, *Thermal performance of seawater desalination systems.* Desalination, 2003. **158**(1): p. 127-142.
108. Omar, W. and J. Ulrich, *Rate of mass deposition of scaling compounds from seawater on the outer surface of heat exchangers in MED evaporators.* CHEMICAL ENGINEERING & TECHNOLOGY, 2006. **29**(8): p. 974-978.
109. Rahman, H., M.N.A. Hawlader, and A. Malek, *An experiment with a single-effect submerged vertical tube evaporator in multi-effect desalination.* Desalination, 2003. **156**(1–3): p. 91-100.

110. Zheng, X., et al., *Seawater desalination in China: Retrospect and prospect.* Chemical Engineering Journal, 2014. **242**(0): p. 404-413.
111. Al-Karaghouli, A. and L.L. Kazmerski, *Energy consumption and water production cost of conventional and renewable-energy-powered desalination processes.* Renewable and Sustainable Energy Reviews, 2013. **24**: p. 343-356.
112. Burgess G and Lovegrove K, *Solar thermal powered desalination: membrane versus distillation technologies*. 2005, Australian National University.
113. Eltawil, M.A., Z. Zhengming, and L. Yuan, *A review of renewable energy technologies integrated with desalination systems.* Renewable and Sustainable Energy Reviews, 2009. **13**(9): p. 2245-2262.
114. Wu, S. and Z. Zhang, *An approach to improve the economy of desalination plants with a nuclear heating reactor by coupling with hybrid technologies.* Desalination, 2003. **155**(2): p. 179-185.
115. Wu, S., *Analysis of water production costs of a nuclear desalination plant with a nuclear heating reactor coupled with MED processes.* Desalination, 2006. **190**(1–3): p. 287-294.
116. Tzen, E. and R. Morris, *Renewable energy sources for desalination.* Solar Energy, 2003. **75**(5): p. 375-379.
117. Andrianne, J. and F. Alardin, *Thermal and membrane processe economics: Optimized selection for seawater desalination.* Desalination, 2003. **153**(1–3): p. 305-311.
118. Karagiannis, I.C. and P.G. Soldatos, *Water desalination cost literature: review and assessment.* Desalination, 2008. **223**(1): p. 448-456.
119. NSW Department of Primary Industries. *Interpreting water quality test results*. Water & Irrigation [Online] 2004 accessed 07/05/2014]; Available from: www.dpi.nsw.gov.au/agriculture/resources/water/quality/publications/results.
120. Ciecko, Z., et al., *Effect of soil contamination by cadmium on potassium uptake by plants.* Polish Journal of Environmental Studies, 2004. **13**(3): p. 333-337.